



AD-A269 647



**Defense Nuclear Agency
Alexandria, VA 22310-3398**



2

DNA-TR-92-101

MHD-EMP Analysis and Protection

**P. R. Barnes, et al.
Energy Division
Oak Ridge National Laboratory
Oak Ridge, TN 37831-6070**

**S DTIC ELECTE D
A SEP 23 1993**

September 1993

Technical Report

CONTRACT No. DE-AC05-84OR21400

Approved for public release;
distribution is unlimited.

20010509013

93-22042



93 9 22 007

Destroy this report when it is no longer needed. Do not return to sender.

**PLEASE NOTIFY THE DEFENSE NUCLEAR AGENCY,
ATTN: CSTI, 6801 TELEGRAPH ROAD, ALEXANDRIA, VA
22310-3398, IF YOUR ADDRESS IS INCORRECT, IF YOU
WISH IT DELETED FROM THE DISTRIBUTION LIST, OR
IF THE ADDRESSEE IS NO LONGER EMPLOYED BY YOUR
ORGANIZATION.**



DISTRIBUTION LIST UPDATE

This mailer is provided to enable DNA to maintain current distribution lists for reports. (We would appreciate your providing the requested information.)

- Add the individual listed to your distribution list.
- Delete the cited organization/individual.
- Change of address.

NOTE:
Please return the mailing label from the document so that any additions, changes, corrections or deletions can be made easily.

NAME: _____

ORGANIZATION: _____

OLD ADDRESS	CURRENT ADDRESS
_____	_____
_____	_____
_____	_____

TELEPHONE NUMBER: () _____

DNA PUBLICATION NUMBER/TITLE	CHANGES/DELETIONS/ADDITIONS, etc.) <small>(Attach Sheet if more Space is Required)</small>
_____	_____
_____	_____
_____	_____

DNA OR OTHER GOVERNMENT CONTRACT NUMBER: _____

CERTIFICATION OF NEED-TO-KNOW BY GOVERNMENT SPONSOR (if other than DNA):

SPONSORING ORGANIZATION: _____

CONTRACTING OFFICER OR REPRESENTATIVE: _____

SIGNATURE: _____

CUT HERE AND RETURN



**DEFENSE NUCLEAR AGENCY
ATTN: TITL
6801 TELEGRAPH ROAD
ALEXANDRIA, VA 22310-3398**

**DEFENSE NUCLEAR AGENCY
ATTN: TITL
6801 TELEGRAPH ROAD
ALEXANDRIA, VA 22310-3398**

REPORT DOCUMENTATION PAGE

Form Approved
OMB No. 0704-0188

Public reporting burden for this collection of information is estimated to average 1 hour per response, including the time for reviewing instructions, searching existing data sources, gathering and maintaining the data needed, and completing and reviewing the collection of information. Send comments regarding this burden estimate or any other aspect of the collection of information, including suggestions for reducing this burden, to Washington Headquarters Service, Directorate for Information Operations and Reports, 1216 Jefferson Davis Highway, Suite 1204, Arlington, VA 22202-4302, and to the Office of Management and Budget, Paperwork Reduction Project (0704-0188), Washington, DC 20503.

1. AGENCY USE ONLY (Leave blank)	2. REPORT DATE 930901	3. REPORT TYPE AND DATES COVERED Technical	
4. TITLE AND SUBTITLE MED-EMP Analysis and Protection		5. FUNDING NUMBERS C-DE-AC05-84OR21400 DNA IACRO 90-825 DNA IACRO 91-825 DNA IACRO 92-805	
6. AUTHOR(S) Paul R. Barnes, Fred M. Tesche, Ben W. McConnell, and Edward F. Vance			
7. PERFORMING ORGANIZATION NAME(S) AND ADDRESS(ES) Oak Ridge National Laboratory Energy Division P. O. Box 2008 Oak Ridge, TN 37831-6285		8. PERFORMING ORGANIZATION REPORT NUMBER	
9. SPONSORING/MONITORING AGENCY NAME(S) AND ADDRESS(ES) Defense Nuclear Agency 6801 Telegraph Road Alexandria, VA 22310-3398 RAEE/Launstein		10. SPONSORING/MONITORING AGENCY REPORT NUMBER DNA-TR-92-101	
11. SUPPLEMENTARY NOTES			
12a. DISTRIBUTION/AVAILABILITY STATEMENT Approved for public release; distribution is unlimited.		12b. DISTRIBUTION CODE	
13. ABSTRACT (Maximum 200 words) A large nuclear detonation at altitudes of several hundred kilometers above the earth distorts the earth's magnetic field and produces a strong magnetohydrodynamic-electromagnetic pulse (MHD-EMP). MHD-EMP is similar to solar geomagnetic storms in its global and low frequency (less than 1 Hz) nature except that it can be more intense with a shorter duration. It will induce quasi-dc currents in long lines. The MHD-EMP induced currents may cause large voltage fluctuations and severe harmonic distortion in commercial electric power systems. Several MHD-EMP coupling models for predicting the induced current on a wide variety of conducting structures are described, various simulation concepts are summarized, and the results from several MHD-EMP tests are presented. To mitigate the effects of MHD-EMP on a facility, long conductors must be isolated from the building, and the commercial power harmonics and voltage swings must be addressed. It is found that facilities can be protected against MHD-EMP by using methods which are consistent with standard engineering practices.			
14. SUBJECT TERMS MHD-EMP Interaction Analysis MHD-EMP Protection Guidelines		Power Line Model Transformer Test	15. NUMBER OF PAGES 86
			16. PRICE CODE
17. SECURITY CLASSIFICATION OF REPORT UNCLASSIFIED	18. SECURITY CLASSIFICATION OF THIS PAGE UNCLASSIFIED	19. SECURITY CLASSIFICATION OF ABSTRACT UNCLASSIFIED	20. LIMITATION OF ABSTRACT SAR

CLASSIFIED BY:

.N/A since unclassified

DECLASSIFY ON:

N/A since unclassified

7. PERFORMING ORGANIZATION NAME(S) AND ADDRESS(ES) (Continued)

**Martin Marietta Energy Systems, Inc.
Oak Ridge National Laboratory
X-10 Laboratory Records Dept.
P. O. Box 2008
Oak Ridge, TN 37831**

9. SPONSORING/MONITORING AGENCY NAME(S) AND ADDRESS(ES)

**Department of Energy
Office of Energy Management
Washington, DC 20585**

PREFACE

The research for this report was jointly sponsored by the Defense Nuclear Agency (DNA) through Interagency Agreement No. 0046-C156-A1 and the Office of Energy Management of the U.S. Department of Energy (DOE) under contract DE-AC05-84OR21400 with Martin Marietta Energy Systems, Inc. The report was prepared by the Energy Division of the Oak Ridge National Laboratory, which is managed by Martin Marietta Energy Systems, Inc. The authors wish to acknowledge and thank Dr. George H. Baker, Lt. Col. Clinton Gordon, and Major Robert J. Launstein of DNA for their interest, support, and review of this work.

The authors also wish to acknowledge and thank John Stovall of the Oak Ridge National Laboratory for his reviews and helpful suggestions during the course of this work.

Accession For	
NTIS CRA&I	<input checked="" type="checkbox"/>
DTIC TAB	<input type="checkbox"/>
Unannounced	<input type="checkbox"/>
Justification	
By	
Distribution /	
Availability Codes	
Dist	Avail and/or Special
A-1	

DTIC QUALITY INSPECTED 1

CONVERSION TABLE

Conversion factors for U.S. Customary to metric (SI) units of measurement.

MULTIPLY $\xrightarrow{\hspace{10em}}$ BY $\xrightarrow{\hspace{10em}}$ TO GET
 TO GET $\xleftarrow{\hspace{10em}}$ BY $\xleftarrow{\hspace{10em}}$ DIVIDE

angstrom	1.000 000 X E -10	meters (m)
atmosphere (normal)	1.013 25 X E +2	kilo pascal (kPa)
bar	1.000 000 X E +2	kilo pascal (kPa)
barn	1.000 000 X E -28	meter ² (m ²)
British thermal unit (thermochemical)	1.054 350 X E +3	joule (J)
calorie (thermochemical)	4.184 000	joule (J)
cal (thermochemical/cm ²)	4.184 000 X E -2	mega joule/m ² (MJ/m ²)
curie	3.700 000 X E +1	*giga becquerel (GBq)
degree (angle)	1.745 329 X E -2	radian (rad)
degree Fahrenheit	$t_k = (t^{\circ}f + 459.67)/1.8$	degree kelvin (K)
electron volt	1.602 19 X E -19	joule (J)
erg	1.000 000 X E -7	joule (J)
erg/second	1.000 000 X E -7	watt (W)
foot	3.048 000 X E -1	meter (m)
foot-pound-force	1.355 818	joule (J)
gallon (U.S. liquid)	3.785 412 X E -3	meter ³ (m ³)
inch	2.540 000 X E -2	meter (m)
jerk	1.000 000 X E +9	joule (J)
joule/kilogram (J/kg) radiation dose absorbed	1.000 000	Gray (Gy)
kilotons	4.183	terajoules
kip (1000 lbf)	4.448 222 X E +3	newton (N)
kip/inch ² (ksi)	6.894 757 X E +3	kilo pascal (kPa)
knap	1.000 000 X E +2	newton-second/m ² (N-s/m ²)
micron	1.000 000 X E -6	meter (m)
mil	2.540 000 X E -5	meter (m)
mile (international)	1.609 344 X E +3	meter (m)
ounce	2.834 952 X E -2	kilogram (kg)
pound-force (lbf avoirdupois)	4.448 222	newton (N)
pound-force inch	1.129 848 X E -1	newton-meter (N·m)
pound-force/inch	1.751 268 X E +2	newton/meter (N/m)
pound-force/foot ²	4.788 026 X E -2	kilo pascal (kPa)
pound-force/inch ² (psi)	6.894 757	kilo pascal (kPa)
pound-mass (lbm avoirdupois)	4.535 924 X E -1	kilogram (kg)
pound-mass-foot ² (moment of inertia)	4.214 011 X E -2	kilogram-meter ² (kg·m ²)
pound-mass/foot ³	1.601 846 X E +1	kilogram/meter ³ (kg/m ³)
rad (radiation dose absorbed)	1.000 000 X E -2	**Gray (Gy)
roentgen	2.579 760 X E -4	coulomb/kilogram (C/kg)
shek	1.000 000 X E -8	second (s)
slug	1.459 390 X E +1	kilogram (kg)
torr (mm Hg, 0° C)	1.333 22 X E -1	kilo pascal (kPa)

*The becquerel (Bq) is the SI unit of radioactivity; 1 Bq = 1 event/s.
 **The Gray (Gy) is the SI unit of absorbed radiation.

CONTENTS

Section	Page
PREFACE	iii
CONVERSION TABLE	iv
FIGURES	vii
1 INTRODUCTION	1
2 THE MHD-EMP ENVIRONMENT	3
2.1 GENERAL	3
2.2 SIMPLIFIED MHD-EMP ELECTRIC FIELDS	5
2.3 ALTERNATE MODELS FOR THE CONDUCTIVE EARTH	6
2.4 SIMILARITIES BETWEEN MHD-EMP AND SOLAR STORMS	12
3 MHD-EMP INTERACTION MODELS	16
3.1 GENERAL	16
3.2 INDUCED EARTH CURRENTS	16
3.3 COLLECTION OF EARTH CURRENTS BY GROUND FACILITIES	17
3.4 CURRENTS INDUCED IN LONG LINES	19
3.4.1 A Single Line Grounded at Both Ends	19
3.4.2 A Periodically Grounded Line	21
3.4.3 Currents in Buried Conductors	23
3.5 CURRENTS IN POWER TRANSMISSION AND DISTRIBUTION LINES	24
3.5.1 Unshielded, Three-Phase Power Lines	24
3.5.2 Considerations for Shielded Three-Phase Power Lines	26
3.6 E_3 COUPLING TO A FACILITY WITH LONG LINES ATTACHED	29
3.7 GROUND CONDUCTOR ISOLATION IN FACILITIES	31
4 MHD-EMP TESTING	34
4.1 OVERVIEW	34
4.2 MHD-EMP SIMULATION CONCEPTS	34

CONTENTS (Continued)

Section	Page
4.2.1 Single Lines	34
4.2.2 Three-Phase Power Lines	39
4.3 MHD-EMP TESTING ON A BURIED FACILITY	43
4.4 MHD-EMP TESTING ON POWER DISTRIBUTION TRANSFORMERS	46
5 MHD-EMP MITIGATION METHODS	57
5.1 GENERAL CONSIDERATIONS	57
5.2 MITIGATION TECHNIQUES FOR COMMERCIAL POWER	58
5.3 OTHER CONDUCTORS	64
5.4 PROTECTION AGAINST HARMONICS	65
6 CONCLUSIONS	66
6.1 SUMMARY	66
6.2 RECOMMENDATIONS FOR MHD-EMP MITIGATION METHODS	67
7 REFERENCES	68
APPENDIX - LIST OF ACRONYMS, ABBREVIATIONS AND SYMBOLS	A-1

FIGURES

Figure	Page
2-1 Orientation of the \mathcal{E} - and B-fields at the earth-air interface.....	4
2-2 Normalized MHD-EMP E-field waveforms.....	7
2-3 Normalized composite MHD-EMP E-field.....	8
2-4 MHD-EMP E-fields for varying earth conductivities under the assumption that $E_{\max} = 10$ V/km for $\sigma = 0.01$ S/m.....	9
2-5 Two-layer earth and transmission line model.....	11
2-6 Geomagnetic storm B-field and resulting E-field at Ottawa, Canada, from ref. 14.	14
2-7 Comparison of MHD-EMP with a geomagnetic storm.....	15
3-1 Geometry of idealized system and MHD-EMP earth-induced E-field.....	18
3-2 Model for a single conductor excited by MHD-EMP.....	20
3-3 A periodically grounded line.....	21
3-4 Circuit model for the periodically grounded line.....	22
3-5 Normalized MHD-EMP-induced current vs. number of tower sections for different line lengths.....	22
3-6 A three-phase, grounded wye electrical power system.....	24
3-7 MHD-EMP-induced current in transmission lines.....	25
3-8 Three-phase line with N towers and overhead shield wires.....	27
3-9 Contours of normalized MHD-EMP-induced current I_c/E_0 (A-km/V) for a 500 kV line with grounded shield wires.....	28
3-10 Buried facility with direct connection of long lines.....	30
3-11 Buried facility with isolation of long lines.....	32
3-12 Geometry of idealized facility and current injection electrodes.....	33

FIGURES (Continued)

Figure	Page
3-13 Normalized current collected by the system as a function of the electrode positions.	33
4-1 An isolated single conductor entering a facility excited by MHD-EMP.	35
4-2 Simulation of MHD-EMP excitation by an equivalent Thevenin circuit.	36
4-3 MHD-EMP simulation with the pulser in series with the line.	37
4-4 MHD-EMP simulation with the pulser across the line.	37
4-5 Configuration of a single line periodically connected to earth.	38
4-6 E_3 excitation of a three-phase power line.	40
4-7 Thevenin equivalent circuit excitation of a three-phase line.	40
4-8 E_3 simulation of a three-phase line with pulser in the transformer neutral conductor.	41
4-9 E_3 simulation of a three-phase line with pulser along the line.	42
4-10 Transformer test configurations.	48
4-11 Diagram of the measurement set up.	49
4-12 Measured current on the primary of transformer T2 for configuration 1A.	50
4-13 Measured current on the secondary of transformer T2 for configuration 1A.	52
4-14 Examples of computed spectra for the measured responses of Figure 4-12.	53
4-15 Measured harmonic content in primary of T2 for configuration 1A with different levels of dc injection.	54
4-16 Measured reactive power demand.	54
4-17 Envelope curve of 60 Hz phase current for configuration 1A.	55
4-18 System relaxation time.	55
5-1 Recommended power system design practices for the primary distribution power line configuration.	59

FIGURES (Continued)

Figure		Page
5-2	Modified recommendations for power system design practices.	62
5-3	Recommended power system design practices for the facility power transformer.	63
5-4	A rotary power conditioner.	63
5-5	Recommended design practice for non-power line conductors.	64
5-6	Protection against harmonics.	65

SECTION 1 INTRODUCTION

This report serves to document a multi-year effort that the Defense Nuclear Agency (DNA) has had with the Oak Ridge National Laboratory (ORNL) in the area of magnetohydrodynamic electromagnetic pulse (MHD-EMP) interaction with ground-based facilities. The overall goal of this project was threefold: to develop a better understanding of the effects on systems; to develop test concepts for the MHD-EMP (also referred to as E_3) environments; and to devise protection methods and guidelines for MHD-EMP.

Under the provisions of this contract, a number of reports documenting different aspects of this effort have been published. Reference [1] discusses MHD-EMP interaction with the electrical power system and develops various calculational models for predicting the levels of MHD-EMP-induced currents in long lines. This reference also discusses the similarity between the E_3 fields and the earth-induced E-fields arising from a solar storm and documents observed effects on the power system during a recent storm.

Reference [2] continues with discussions of MHD-EMP effects on the electrical power system, and discusses methods of mitigating the effects of this environment. In addition, guidelines for testing facilities to determine the effects of MHD-EMP and to validate the mitigation methods are discussed.

An experimental program for determining the behavior of electrical power distribution transformers was conducted under this effort, and is documented in [3]. This test illustrated the saturation properties of distribution transformers, and presents data on the consequent reactive power demand on generation equipment. A second experimental program for determining E_3 effects on a large, ground-based facility is described in [4]. This test involved injecting large quasi-dc currents onto the exterior of the facility and into the electrical power system to observe possible effects.

In addition to these formal reports, three technical presentations have been made which stem from the work conducted under this effort. Presentations [5], [6], and [7] described the work of refs. [1], [2], and [3], respectively.

In the present report, the important techniques, observations and conclusions from these previous reports are summarized. After this introduction, Section 2 briefly discusses the

MHD-EMP environment used for these studies. As this effort was not chartered to develop new MHD-EMP environments, the work of other investigators was used to obtain estimates of the earth-induced E-fields. Much of the work performed in this study, however, is insensitive to the details of the E_3 environmental levels, since the results are quoted in a normalized manner.

The various MHD-EMP interaction models developed and used in this study are summarized in Section 3. Due to the low-frequency nature of the MHD-EMP excitation (typically below 1 Hz), these models essentially involve dc circuit modeling concepts. Complications can arise, however, when electrically complex conducting structures, such as a three-phase power line with a periodically grounded neutral conductor, are considered.

Section 4 summarizes the MHD-EMP testing issues that have been considered under this effort. This includes the development of test concepts and recommendations, and the results of actual E_3 testing of facilities and transformers. A brief summary of the mitigation measures appropriate for MHD-EMP are then presented in Section 5.

Section 6 concludes this report with a summary of the work and recommendations for future work to resolve remaining issues.

SECTION 2 THE MHD-EMP ENVIRONMENT

2.1 GENERAL.

As discussed in ref. [8], the MHD-EMP or E_3 environment arises from a variation of the earth's magnetic field caused by a high-altitude nuclear detonation. The interaction of this time-varying magnetic flux (B-field) with the imperfectly conducting ground causes a transient electric field to be induced on the surface of the earth, in a manner analogous to that occurring in a geomagnetic storm [9]. For a transient tangential B-field on the surface of a homogenous earth, the corresponding electric field tangential to the earth is expressed as

$$E(t) = \frac{1}{\sqrt{\pi\sigma\mu}} \int_{-\infty}^t \frac{1}{\sqrt{t-t'}} \frac{\partial B(t')}{\partial t'} dt' \quad (2-1)$$

where σ is the earth electrical conductivity and $\mu = 4\pi \times 10^{-7}$ H/m is the permeability of the soil [8]. As shown in Figure 2-1, the E- and B-fields are mutually orthogonal and are both parallel to the earth's surface. The time variation of the resulting E_3 -field is much slower than the early-time E_1 HEMP environment. Typical waveform times for the MHD-EMP environment are on the order of several hundreds of seconds.

Within the earth, a volume current density $J(t)$ exists and is related to the electric field within the earth as $J(t) = \sigma E(t)$. Both of these time domain quantities decay in amplitude and become temporally smoother at locations deep within the earth. In the frequency domain, the spectra of these quantities vary exponentially with depth into the earth as $e^{-z/\delta}$, where δ is the skin depth of the soil, defined as $\delta = 1/\sqrt{\pi f \mu \sigma}$. If there are long conductors connected to the earth at two or more points, or in continuous direct contact with the ground, a portion of this earth-induced current can flow into the conductors. These induced currents have the potential of disrupting electrical power systems and communications systems, and are the focus of this study.

The E_3 environment may be divided into two parts, based on the postulated mechanisms of production [8]. The first part, for times between $1 \leq t < 10$ sec, arises from the initial nuclear burst and its interaction with the earth's magnetic field. This part is referred to as the blast-wave component. At later times for $10 \leq t < 500$ sec, a second contribution to the geomagnetic field variation arises due to the late-time atmospheric heave.

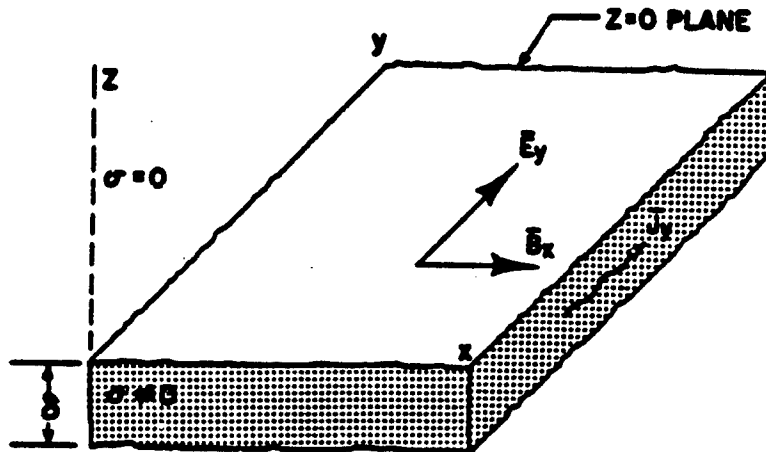


Figure 2-1. Orientation of the E- and B-fields at the earth-air interface.

The preliminary E_3 environment used in refs. [8] and [10] for an MHD-EMP assessment of commercial power networks was based on early measurements of the geomagnetic fluctuations measured on Johnston Island during the Fishbowl test series. These measurements were used in conjunction with the MICE computer code to provide a numerical simulation of the time development of the disturbed atmosphere, as described in ref. [11].

Recent refinements in the theory of MHD-EMP production have led to an alternate computer model for predicting the blast-wave environment [12]. In addition, there are some preliminary results for the late-time heave component of the E_3 environment. This work has been used to develop an updated composite MHD-EMP environment, which can be used to estimate the behavior of induced currents in long transmission and distribution lines, and has been used in refs. [1] and [2] for studies of MHD-EMP effects on electrical power systems.

According to [12], a simplified way of viewing the early-time, blast-wave E_3 environment is to consider a quasi-static problem in which a magnetic dipole moment at the burst point is used to represent a perturbation source for the geomagnetic field. This dipole is oriented in a direction opposing the earth's magnetic field. Below this dipole, at an altitude of about 110 km, is a conducting region, or patch, which is created by downward-streaming x-rays from the detonation. For this model, the x-ray patch is assumed to be perfectly conducting, with no penetration by the early-time magnetic field. However, the B-field from the dipole moment does reach under the patch by flowing out around the ends of the patch and

reconnecting in the region between the patch and the ground. In some of the MHD-EMP literature, this process is variously described as "propagation" or "diffraction," but since these are nominally high-frequency concepts and the MHD-EMP is quasi-static in nature, the use of these terms is avoided.

2.2 SIMPLIFIED MHD-EMP ELECTRIC FIELDS.

For studies of E_3 effects on systems, it is the E-field that is of prime concern, and this can be computed from Eq.(2-1), once the time and spatial variation of the P-field is known. Under the x-ray patch, the blast-wave E-field is observed to be smaller than outside this shielded region. The field is oriented primarily in the west-east direction and does not appear to vary drastically with position. Outside the shielded region, the E-field appears to fall off with distance away from the burst, with the largest field occurring just outside the x-ray shield.

For the purpose of estimating the coupling of MHD-EMP environments to power systems, several different E-field waveforms have been used [1]. Figure 2-2a presents a typical waveform for the early-time blast component of the E-field on the earth's surface. This component of the MHD-EMP environment, denoted by $E_0(t)$, is normalized by a factor E . Slight differences in the normalized waveform shape are noted for observation locations outside of the x-ray patch compared with locations under the patch, but these are neglected here. The normalization factor E_{\max} depends on many factors, including the burst yield and other parameters, the exact observer location, and the earth's electrical conductivity.

Figure 2-2b presents a typical late-time heave contribution to the MHD-EMP E-field. As in the previous figures, this waveform is also normalized to unity by a factor E_{\max} which is different from that for the blast-wave component. This component of the MHD-EMP environment is believed to be strongest directly under the burst, falling off rapidly as the observer moves away from ground zero.

The total MHD-EMP E-field on the ground consists of a suitable combination of Figures 2-2a and 2-2b, depending on the actual location of the observer. For some locations the late-time component of the environment will be very small, but for others it can be substantial. As an example of such a composite MHD-EMP waveform, Figure 2-3a presents a complete normalized waveform and its frequency-domain spectral magnitude is shown in Figure 2-3b. Note that most of the spectrum is located well below 1 Hz. For power systems,

this implies that the MHD-EMP waveform appears as a quasi-dc signal, and that dc circuit modeling concepts will be appropriate for calculating system responses.

For reasons mentioned previously, the MHD-EMP E-field vector direction depends on the burst location relative to the magnetic north pole. As in the case of solar geomagnetic storms, for burst locations near the north pole, much of the earth's surface experiencing the MHD-EMP environment sees a predominantly east-west E-field. Consequently, for the study in ref. [1], the direction of the E-field is assumed to be east-west.

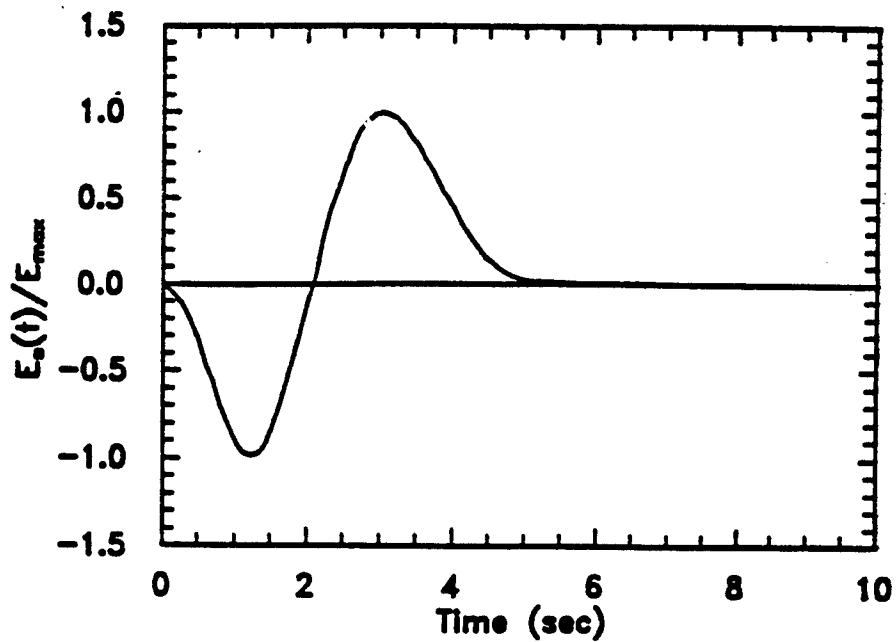
For some calculational procedures, an explicit expression for the waveforms shown in Figures 2-2a and 2-2b is useful. Such expression may be obtained by fitting the waveform components to a suitable functional form, and this is discussed in more detail in ref. [1].

As noted in Eq.(2-1), the magnitude of the E_3 environment depends on the electrical conductivity of the earth. As an example of the range of possible E-field amplitudes, a nominal E_3 environment of 10 V/km has been assumed for an earth conductivity of $\sigma = 0.01$ S/m. Figure 2-4 shows the resulting E-field waveforms as the earth conductivity is decreased from 0.01 to 5.0×10^{-5} S/m.

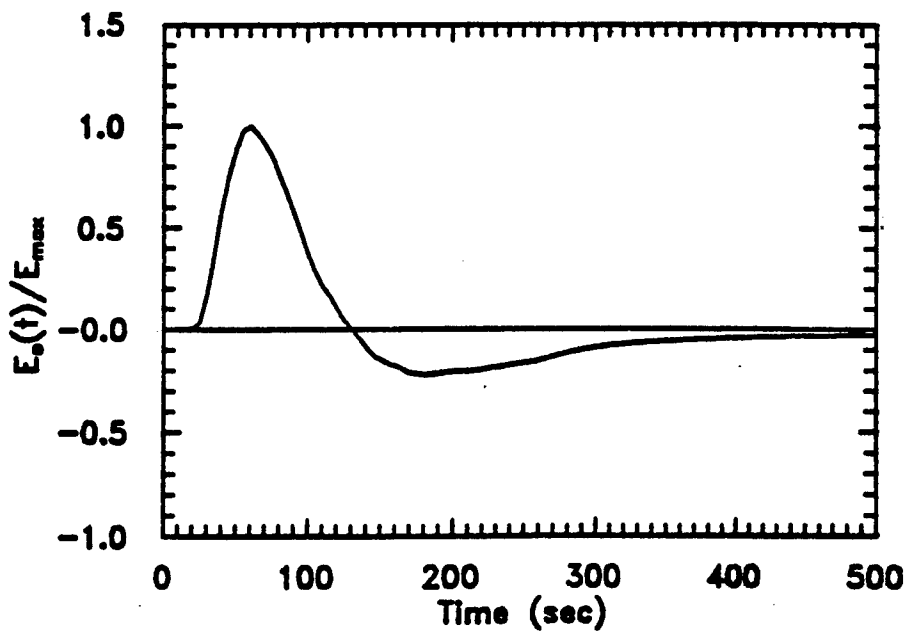
2.3 ALTERNATE MODELS FOR THE CONDUCTIVE EARTH.

The derivation of Eq.(2-1) for the E-field is based on the assumption that the earth is a uniform half-space with conductivity σ . In reality, the earth is inhomogeneous, with the possibility of many different layers, each having different conductivities. Furthermore, there can be large changes in the conductivity in the lateral direction, especially at the coastline, where the conductivity changes from that of soil to sea water.

Frequently, the surface conductivity is different from that deep in the earth. Due to the high frequency content in the early-time E_1 HEMP environment, the surface conductivity is most important in determining the total E_1 -field above the surface. However, the lower frequency E_3 fields are typically more sensitive to the layered structure deep within the earth. Alternate calculational models are available for the E_3 fields which take into account the deep earth structure. These will be described in this section. It must be kept in mind, however, that these models require a knowledge of the deep earth conductivity and its variations to be

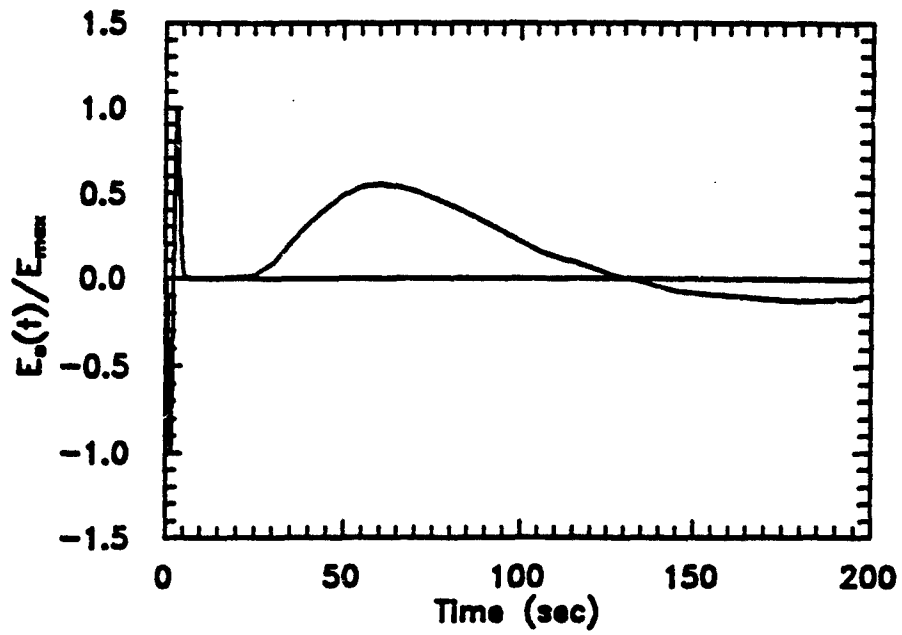


a. Normalized early-time, blast wave contribution

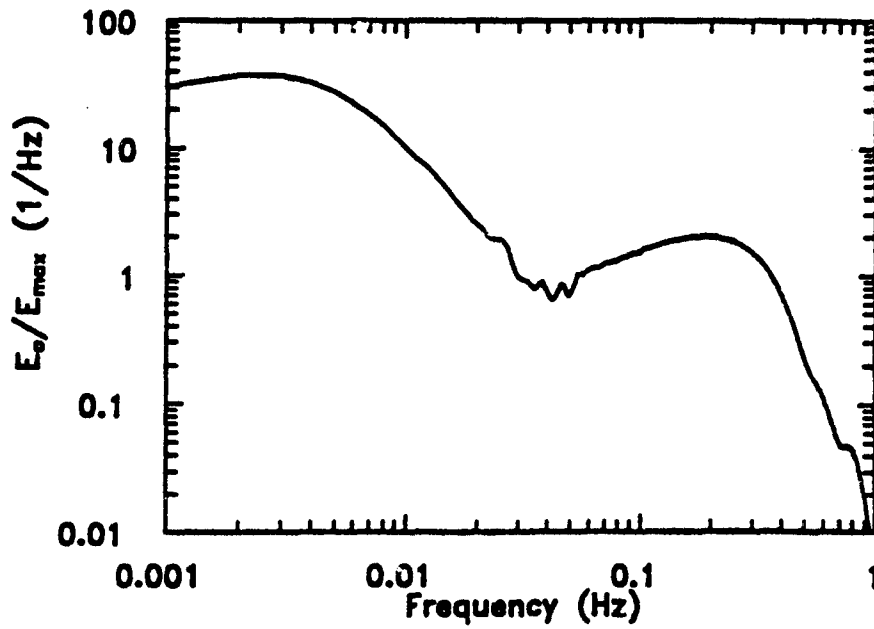


b. Late-time, heave contribution

Figure 2-2. Normalized MHD-EMP E-field waveforms.



a. Time-domain waveform



b. Frequency-domain spectrum magnitude

Figure 2-3. Normalized composite MHD-EMP E-field.

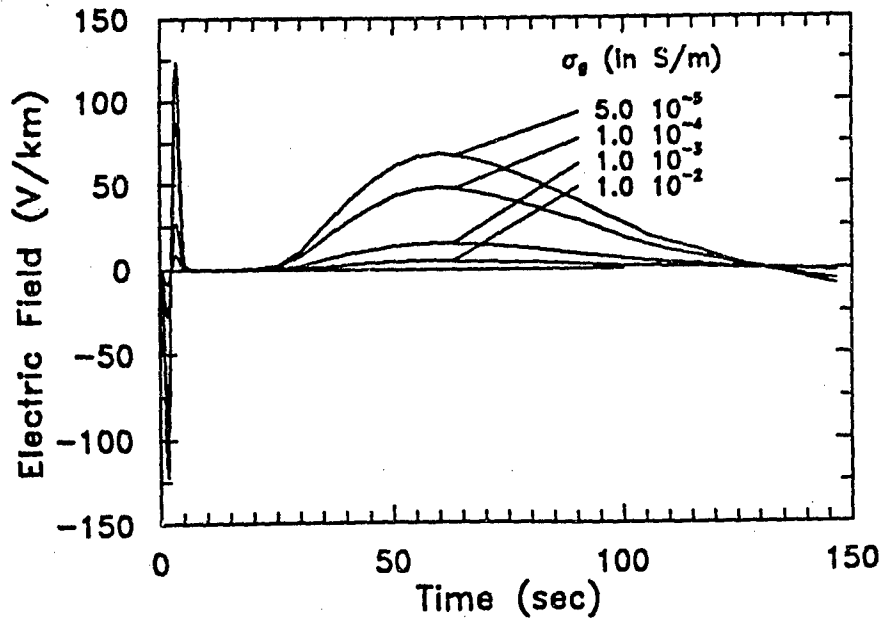


Figure 2-4. MHD-EMP E-fields for varying earth conductivities under the assumption that $E_{max} = 10$ V/km for $\sigma = 0.01$ S/m.

applied. Such data may not be available in practical cases of interest, and the resulting errors of applying these models with improperly chosen ground data can provide field estimates that are just as inaccurate as those obtained by using the simple, homogeneous earth model.

To develop a model for a more realistic earth, first consider the case of a simple lossy half-space. As discussed by Wait [13], the frequency domain relationship between the total E- and H-field on the surface of the earth is defined by a surface impedance Z_s as

$$E = Z_s H . \quad (2-2)$$

For a single, homogeneous earth, the surface impedance is given in [13] as

$$Z_s = \sqrt{\frac{j\omega\mu}{j\omega\epsilon + \sigma}} \approx \sqrt{\frac{j\omega\mu}{\sigma}} . \quad (2-3)$$

Noting that $B = \mu H$, the expression in Eq.(2-2) can be written in terms of the spectrum of the time derivative of the B-field $j\omega B$ as

$$E = T(j\omega) j\omega B , \quad (2-4)$$

where the transfer function $T(j\omega)$ is given by

$$T(j\omega) = \frac{1}{j\omega\mu} Z_s = \frac{1}{\sqrt{j\omega\mu\sigma}} \quad (2-5)$$

for the homogeneous earth. As discussed in the Appendix of ref. [8], this frequency-domain expression leads directly to the time-domain convolution operation of Eq.(2-1).

An alternative to evaluating Eq.(2-1) directly is to compute the B-field spectrum by performing a Fourier transform on the assumed known transient B-field on the earth's surface, and then using Eqs.(2-4) and (2-5) to compute the E-field spectrum. The final transient response is then calculated by performing an inverse Fourier transform.

Consider now the case of the two-layer earth shown in Figure 2-5. This consists of a single layer having a thickness d and electrical parameters σ_1 , ϵ_1 , and μ_1 , and is located over an otherwise homogeneous earth described by parameters σ_2 , ϵ_2 , and μ_2 . The E/H relationship on the surface can be computed using the transmission line analogy shown in the figure, and this gives the surface impedance as

$$Z_s = \frac{E_s}{H_s} = Z_c \left(\frac{Z_L + Z_c \tanh(\gamma d)}{Z_c + Z_L \tanh(\gamma d)} \right), \quad (2-6)$$

where the load impedance Z_L is used to represent the surface impedance of the layer 2 and is given by Eq.(2-3) with the values of μ and σ appropriate for layer 2. The term Z_c is the characteristic impedance of the line and this is given by the impedance of Eq.(2-3) with μ and σ for layer 1. The propagation constant γ for region 1 is given by

$$\gamma = \sqrt{j\omega\mu(j\omega\epsilon + \sigma)} \approx \sqrt{j\omega\mu\sigma} \quad (2-7)$$

where again μ and σ are those for layer 1. Note that in these expressions, low-frequency approximations have been made, and this shows that the dielectric constants of the regions are unimportant. Once the Z_s term is evaluated, the E field follows directly from Eqs.(2-4) and (2-5) as

$$E(j\omega) = T(j\omega) j\omega B(j\omega) = \frac{1}{j\omega\mu} Z_c \left(\frac{Z_L + Z_c \tanh(\gamma d)}{Z_c + Z_L \tanh(\gamma d)} \right) j\omega B(j\omega) \quad (2-8)$$

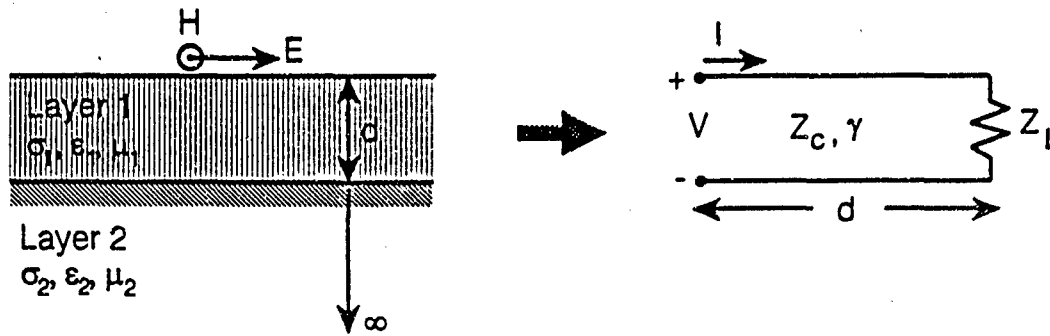


Figure 2-5. Two-layer earth and transmission line model.

For a general, n -layer earth, Eq.(2-6) also can be used to determine the surface impedance. This is done by using the transmission line analogy on a layer-by-layer basis, starting with the deepest layer and moving towards the surface. For any given layer, the computed surface impedance of the previous layer forms the load impedance in Eq.(2-6), and the calculated Z_s then becomes the load impedance for the next layer. Ultimately, a complex frequency domain expression between E and H on the surface results, involving a knowledge of each of the layer thicknesses and parameters μ and σ . As in the case of a single layer earth, the transient response of the E -field is then obtained by performing a numerical inverse Laplace transform.

It is of interest to develop a time-domain representation of the earth-induced E -field similar to that of Eq.(2-1) for the case of the two-layer earth. For the earth model shown in Figure 2-6, Eq.(2-8) can be transformed into the time domain to provide the convolution integral representation for the E -field as

$$E(t) = \int_{-\infty}^t T(t-t') \frac{\partial B(t')}{\partial t'} dt' \quad (2-9)$$

The time domain kernel T in Eq.(2-9) is essentially the inverse Fourier transform of the transfer function $T(j\omega)$ in Eq.(2-8). Using F^{-1} to represent the inverse Fourier transform, this kernel may be expressed as

where $\Gamma = \frac{\sqrt{\sigma_1} - \sqrt{\sigma_2}}{\sqrt{\sigma_1} + \sqrt{\sigma_2}}$ and $k = d^2 \mu_0 \sigma_1$ for the case when the permeabilities μ of each layer are equal to μ_0 . The term d represents the thickness of the layer. In this manner, the convolution integral for the two-layer earth becomes

$$E(t) = \frac{1}{\sqrt{\mu_0 \sigma_1 \pi}} \int_{-\infty}^t \frac{1}{\sqrt{t-t'}} \left[\frac{1 + \Gamma e^{-k/(t-t')}}{1 - \Gamma e^{-k/(t-t')}} \right] \frac{\partial B}{\partial t'} dt' \quad (2-10)$$

This latter expression can be used just as easily as Eq.(2-1) for determining the E-field for a two layer earth. Extension of this expression to a more general, n-layer has not been attempted, but may be possible.

2.4 SIMILARITIES BETWEEN MHD-EMP AND SOLAR STORMS.

The MHD-EMP environment is similar to that encountered in naturally occurring geomagnetic storms. Consequently, it is useful to look to the several reported power system malfunctions which have been ascribed to these storms [1]. Doing this can provide an indication of possible MHD-EMP effects on electrical power systems.

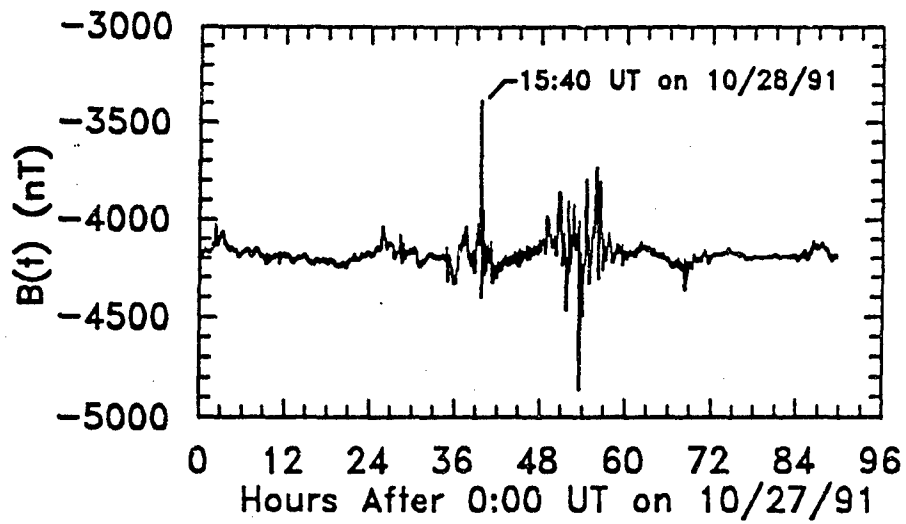
On October 28 and 29, 1991, a major geomagnetic storm occurred. This was given a K-Index of 9 from readings made in Boulder, Colorado, and in Loring, Maine. The storm began at 1540 universal time (1040 EST, 0940 CST, 0840 MST, 0740 PST) on October 28. A number of geomagnetic observatories across the US and Canada recorded the fluctuations of the geomagnetic field during this event and can provide data. Of particular interest are the data from the Canadian Geological survey of Canada [14], as the data are available at 10 second measuring intervals. Other data, such as those available from the U.S. Geological Survey, are typically available only with a one minute time resolution [15].

Figure 2-6a presents the measured East-West geomagnetic field at the Ottawa Magnetic Observatory, as provided by van Beek [14]. These data are plotted as a continuous record for a three-day period, starting on 10/27/91. The vertical axis is the absolute magnetic field (i.e., the static geomagnetic field plus a small time-varying component) in units of nano-Teslas. The onset of the geomagnetic storm is defined to be at about 15:40 universal time on October 28, and this time is indicated on the plots.

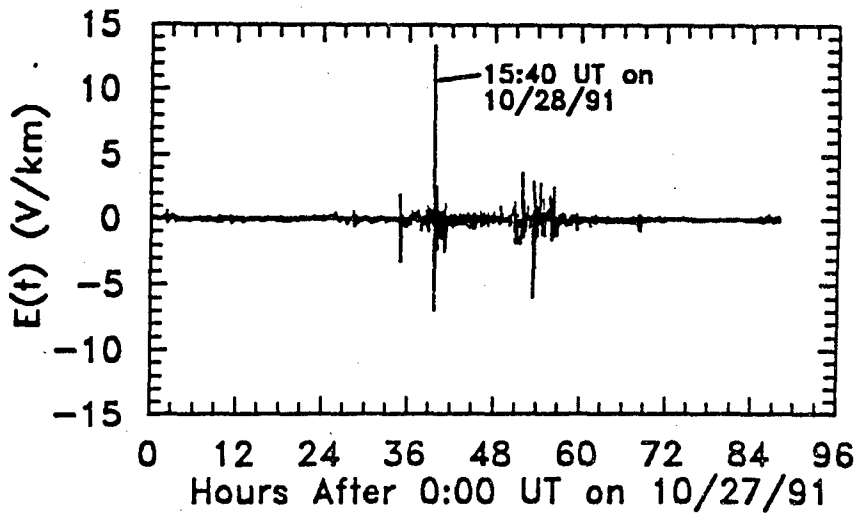
For a simple, homogeneous conducting half-space earth model, the North-South electric field corresponding to this magnetic field may be calculated by numerically evaluating the convolution integral of Eq.(2-1). Assuming an electrical conductivity of $\sigma = 0.0001$ S/m., Figure 2-6b presents the resulting calculated E-fields for this storm. Shown in this figure is a 14 V/km spike in the E-field which caused several problems in power systems across the U.S. [1]. The actual earth conductivity varies depending on the location within in the country. Consequently, different earth conductivities may be possible. The value of σ chosen here is to illustrate possible E-field responses.

To observe in better detail the behavior of the earth-induced E-fields at the onset of the storm, Figure 2-7 presents the North-South E-fields on an expanded time scale in minutes after 15:30 universal time on October 28.

Also shown in this figure is a plot of the normalized composite MHD-EMP E-field, similar to that shown in Figure 2-3a. The MHD-EMP waveform has been normalized here to have the same peak amplitude of about 14 V/km. Note that there is a remarkable similarity between these two waveforms, with an early-time spike, followed by a later-time component. From these observations of geomagnetic storm effects on the power system, it is reasonable to conclude that the power system would respond to a MHD-EMP event.



a. Measured East-West B-field



b. Computed North-South E-field

Figure 2-6. Geomagnetic storm B-field and resulting E-field at Ottawa, Canada, from ref. 14.

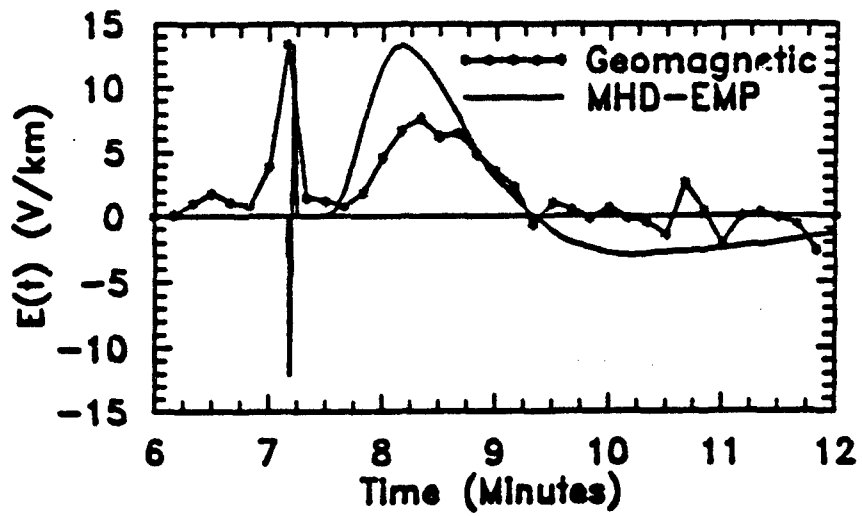


Figure 2-7. Comparison of MHD-EMP with a geomagnetic storm.

SECTION 3

MHD-EMP INTERACTION MODELS

3.1 GENERAL.

The earth-induced currents produced by a MHD-EMP environment arising from a high altitude nuclear burst can interact with a system in several manners. One way is by a direct collection of the earth currents by the system. Another coupling mechanism is by long electrical conductors collecting the earth current and injecting it onto the exterior of the system. Once the current is flowing on the system enclosure, it can diffuse into the interior and may cause disturbances in internal equipment. A third coupling mechanism is by a direct injection of the E_3 currents into a system by penetrating conductors, such as the ac power or telephone lines.

As in the case of the early-time E_1 HEMP environment, it is believed that the largest E_3 excitation of a system arises from the conducting penetrations. In this section, various calculational models are described, and estimates of the injected current levels for different types of conducting penetrations are given. In addition, the other two modes of system excitation are discussed, and estimates of the E_3 currents collected by the system exterior are provided. Of special interest is the possible requirement of maintaining an isolation zone for long conductors conducting E_3 currents to the system.

3.2 INDUCED EARTH CURRENTS.

The MHD-EMP E-field produced by variations in the geomagnetic field in accordance with Eq.(2-1) acts on the conducting earth and induces a volumetric current density J within the earth. This current is given by Ohm's law as $J = \sigma E$. For a nominal E_3 environment of 10 V/km and an earth conductivity of $\sigma = 0.001$ S/m, the resulting current density is only $10 \mu\text{A}/\text{m}^2$. Very long electrical conductors, however, can collect a portion of this current from the earth, and in certain cases this can result in line currents on the order of hundreds of amps.

The induced current density, as well as the E-field, attenuates exponentially with depth into the soil. At the upper frequency limit of the E_3 spectra (see Figure 2-3b) of about $f = 1$ Hz, the skin depth is $\delta = 1/\sqrt{\pi f \mu \sigma} \approx 16,000$ m. Thus, for practical purposes, the current in the ground can be considered as being uniformly distributed.

3.3 COLLECTION OF EARTH CURRENTS BY GROUND FACILITIES.

A starting point for understanding the coupling of the E_3 environment to a system is to consider the collection of the ground current by a shallowly buried system, as shown in Figure 3-1. Because of the large skin depth within the earth, the shallowly buried system experiences the same E-field as does one located on the surface. If the system is assumed to be more highly conducting than the surrounding earth, it will distort the local E-field and cause a current to be collected on its front surface, pass over the system, and then exit off the back side.

As illustrated in Figure 3-1a, a buried system is approximated by a perfectly conducting hemisphere of radius a and a quasi-static E-field in the earth of magnitude E_0 . To compute the earth induced current collected by the system, it is sufficient to determine the local E-field around the system, since the current in the earth is proportional to this field. Once the normal component of E is found on the bottom part of the hemisphere, the current density flowing onto the system can be computed using Ohm's law.

This problem is simplified by using symmetry arguments which permit the consideration of the geometry shown in Figure 3-1b. This is a complete sphere immersed in an initially uniform E-field and is a classical EM textbook problem [16]. On the surface of the sphere, the current density flowing into the sphere is given by

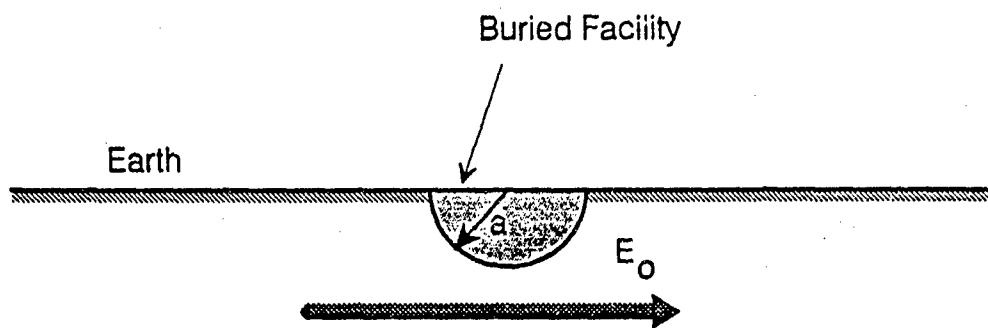
$$J_r = \sigma E_r|_{r=a} = 3\sigma E_0 \cos \theta, \quad (3-1)$$

and the total current flowing into the front side of the hemisphere is by

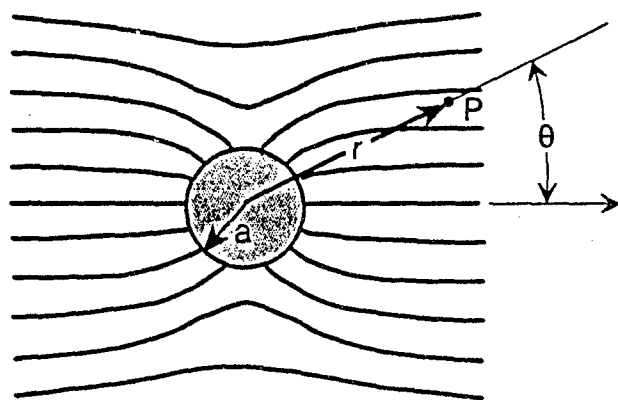
$$I = \int_0^{\pi/2} \int_0^{2\pi} J_r a^2 \sin \theta \, d\theta \, d\phi = \frac{3\pi}{2} a^2 \sigma E_0, \quad (3-2)$$

where a is the radius of the hemisphere. Note that this is three times the current flowing through a half-disk having the same cross sectional area as the hemisphere.

As a numerical example of the magnitude of the collected current for this system, consider the case of a conducting earth of $\sigma = 0.001$ mhos/m and a nominal E_3 field of 10 V/km discussed previously. For a large facility having a radius of 20 m, the total collected current on one side of the system is only about 0.02 A. This current is small and it is doubtful that it would cause any serious problems to equipment within the system enclosure, provided it flows primarily on the shield or structural metal.



a. System geometry



b. Current flow around buried system

Figure 3-1. Geometry of idealized system and MHD-EMP earth-induced E-field.

3.4 CURRENTS INDUCED IN LONG LINES.

The MHD-EMP electric field described in the previous section is capable of inducing currents in long sections of electrical conductors. Unlike the early-time E_1 HEMP environment, which can induce large currents in conductors not connected to the ground, the E_3 environment will induce currents in the lines only if they are electrically connected to the earth at two or more locations. This is due to the quasi-static nature of the MHD-EMP fields. In this section, the models for several different conductor configurations developed in ref. [1] are reviewed and the computed MHD-EMP-induced currents summarized.

3.4.1 A Single Line Grounded at Both Ends.

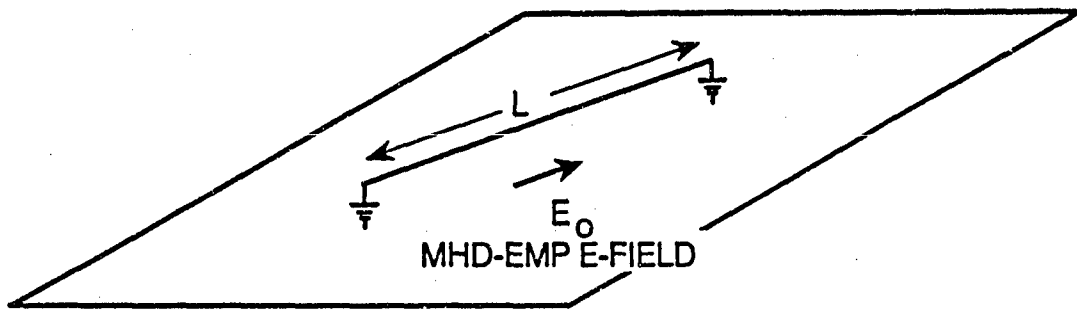
Figure 3-2a shows an example of a conducting, above-ground, line of length L that is connected to the earth at both ends. With the line absent, the earth-induced E-field creates a uniform current density J_g in the earth. When the conducting line is connected to the earth, a fraction of this earth current will be collected by the line, and this results in the current I flowing in the line.

For this simple conductor configuration, the induced line current can be calculated using the simple dc circuit model of Figure 3-2c. As discussed in [1], the effect of the E-field appears as a voltage source ($V = E_0 L$) in series with the line. The resulting current I flowing in the line is given by

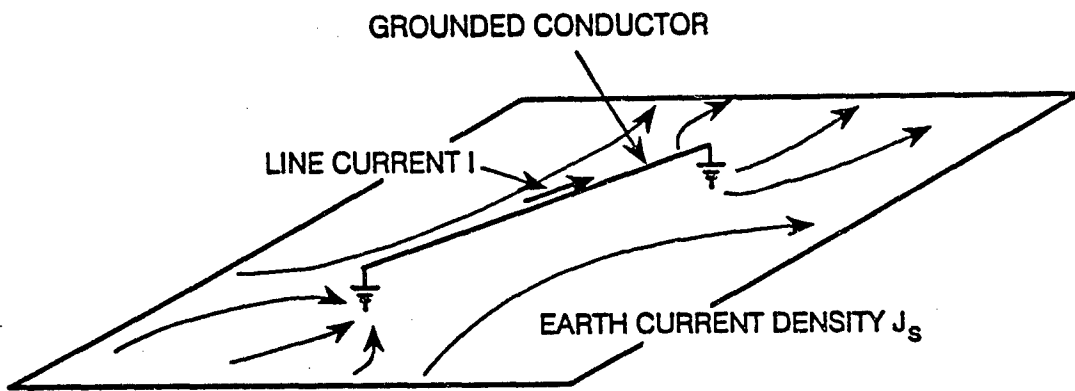
$$I = \frac{E_0 L}{R_{f1} + R_{f2} + r_L L} \quad (3-3)$$

where R_{f1} and R_{f2} represent the grounding (footing) resistances at each end of the line and r_L is the per-unit-length resistance of the conductor, and L is the length of the conductor.

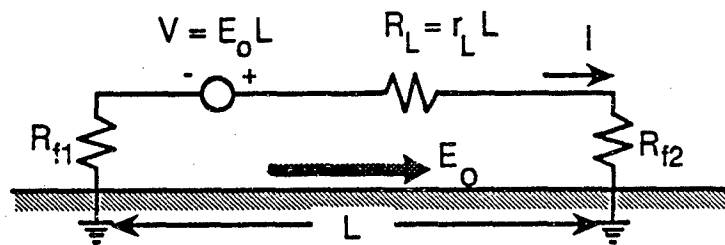
This model is useful for determining the current induced on long lines that can be grounded to the earth. Examples include non-signal conductors such as fences or structural members, the outer shield of a coaxial communications cable, or certain configurations of a three-phase electrical power system which has grounded wye transformers. This latter case will be discussed further in Section 3.5



a. Physical configuration



b. Induced current distribution



c. Circuit model

Figure 3-2. Model for a single conductor excited by MHD-EMP.

3.4.2 A Periodically Grounded Line.

Frequently, a long line will be connected to the earth at several locations along the line. Such is the case with an overhead neutral or shield conductor in a power transmission system, which is connected electrically to each tower. This configuration is shown in Figure 3-3. Each tower has a resistance to ground denoted by R_T . The resistance to ground of the neutral conductor at each end is denoted by R_f . The transformer windings and phase conductors are shown in this figure, but because they are connected to the earth at only one location, they do not enter into the dc analysis for the induced current I_n flowing in at the end of the neutral wire. The term r_s is the per-unit-length resistance of the grounded neutral wire.

Reference [1] discusses the MHD-EMP coupling to this line in detail, and develops the dc circuit model shown in Figure 3-4 for computing the neutral conductor current. This analysis involves a dc loop analysis for the network which has an individual voltage source arising from the E_3 field in each loop. In this reference, calculations for the induced neutral current have been described for typical power line configurations. As an example of these results, Figure 3-5 presents a family of curves of the normalized neutral current I_n/E_0 vs. the number of tower sections in a neutral line having a specified length. Data for line lengths of 15, 10, 5, and 1 km are presented. Additional information on the details of the line parameters used may be found in the reference.

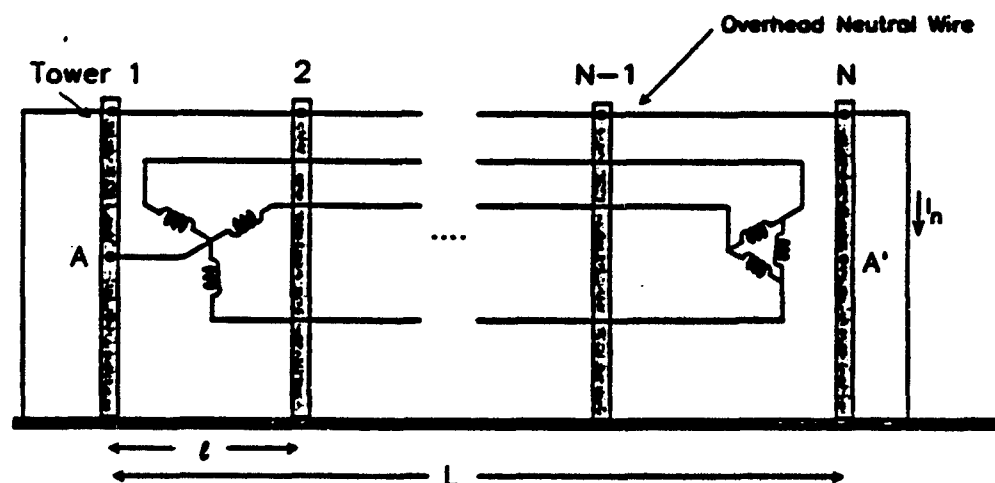


Figure 3-3. A periodically grounded line.

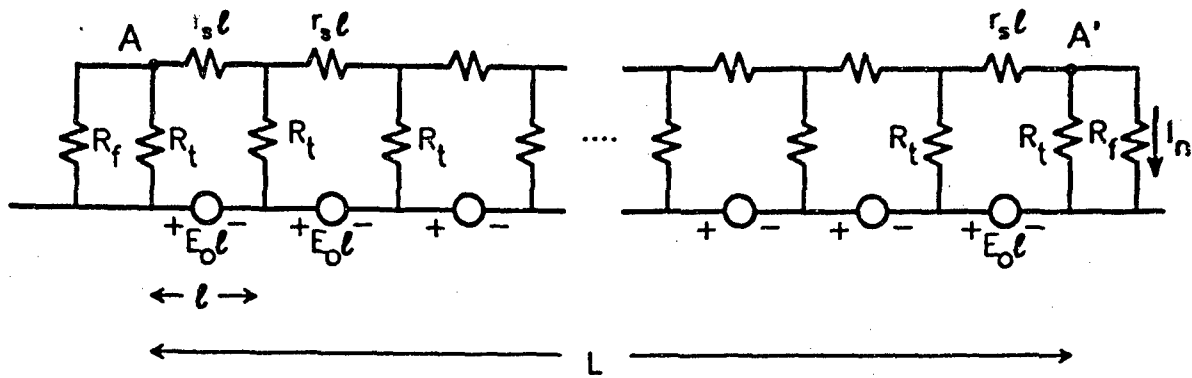


Figure 3-4. Circuit model for the periodically grounded line.

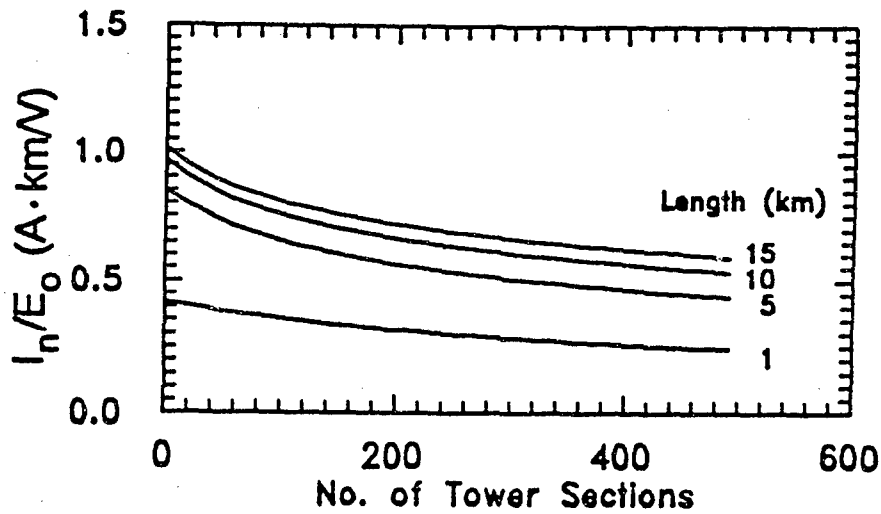


Figure 3-5. Normalized MHD-EMP-induced current vs. number of tower sections for different line lengths.

From the results in [1], it is clear that the MHD-EMP current induced in the grounded line is reduced due to the shunting effects of the towers. For the line having the typical 12 kV distribution line parameters, it was found that there is a reduction of about 30% in the MHD-EMP current induced in the neutral conductor.

3.4.3 Currents in Buried Conductors.

In the limiting case of there being many grounding locations along a line, the problem approaches that of a conductor in continuous contact with the earth. In this case, instead of using a discrete circuit analysis model for determining the line responses, it is possible to use a continuous, analytical model. As developed in [1], the voltage and current distribution on a conductor in contact with the earth are similar to those of a transmission line excited by an incident E-field, with several simplifications arising due to the quasi-static nature of the problem. As a result, analytical expressions for the responses can be obtained.

For a buried line having a per-unit-length resistance of r_s , Ω/m and a per-unit-length conductance to the ground of g_t , S/m, ref. [1] develops the following expression for the current I_n flowing at the end of the line:

$$I_n = \frac{E_o L (1 - e^{-\alpha L})^2}{r_s L (1 - e^{-\alpha L})^2 + \alpha L R_f (1 - e^{-2\alpha L})} \quad (3-4)$$

Here, the parameter $\alpha = \sqrt{r_s g_t}$, and it is assumed that each end of the buried line is terminated in resistances R_f at the ends. This expression provides a current at the end of the line which is smaller than that occurring for the same line which is not in direct contact with the earth.

This last equation can also be applied to the case of a large number N of discrete grounding points having a resistance R_f by defining the per-unit-length conductance g_t as

$$g_t = \frac{N}{R_f L} \quad (\text{S/m}). \quad (3-5)$$

In this manner, the parameter α is

$$\alpha = \sqrt{\frac{N r_s}{R_f L}} \quad (1/m). \quad (3-6)$$

3.5 CURRENTS IN POWER TRANSMISSION AND DISTRIBUTION LINES

3.5.1 Unshielded, Three-Phase Power Lines.

Reference [1] has also discussed the behavior of E_3 -induced currents in transmission and distribution lines having the grounded wye configuration shown in Figure 3-6. Because of the balanced nature of this three-phase system, the earth connections at each end of the line can be made without affecting the normal operation of the power system. The circuit model of Figure 3-2c is appropriate in this case, if the per-unit-resistance r_L represents the parallel combination of the three phase conductors, and the footing resistances R_{F1} and R_{F2} are assumed to contain the dc resistances of the transformer windings R_y at each end of the line.

As discussed in [1], the various resistance values for a power transmission or distribution system depend on the voltage class of the power system being considered. To obtain an indication of possible current responses for different line configurations, several line classes have been examined in [1], and plots of possible MHD-EMP induced currents in the transformer neutrals have been presented.

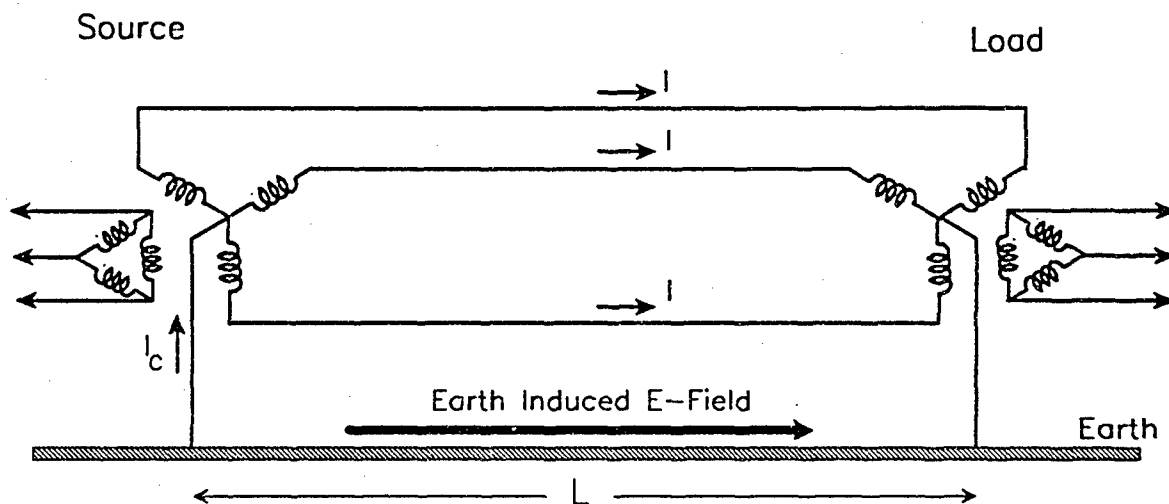


Figure 3-6. A three-phase, grounded wye electrical power system.

As an example of the calculated responses of [1], Figure 3-7, illustrates the behavior of the normalized MHD-EMP-induced neutral current. This is shown as a function of the line length L , for lines in the 138-, 345-, and 500-kV classes. For these types of power lines, an effort is made to keep the transformer neutral grounding resistance low, usually between 0.5 to 1.0 Ω . For the study in [1], the footing resistance for these lines was assumed to be $R_f = 0.75 \Omega$.

Eq. (13) indicates that for very long lines the induced current is dependent only on the per-unit-length line resistance as $I_c/E_o \rightarrow I/r_L$. This current limiting is apparent in the curves in Figure 3-7. For the transmission and distribution lines considered in [1], Table 1 summarizes the peak MHD-EMP-induced currents which occur for very long lines.

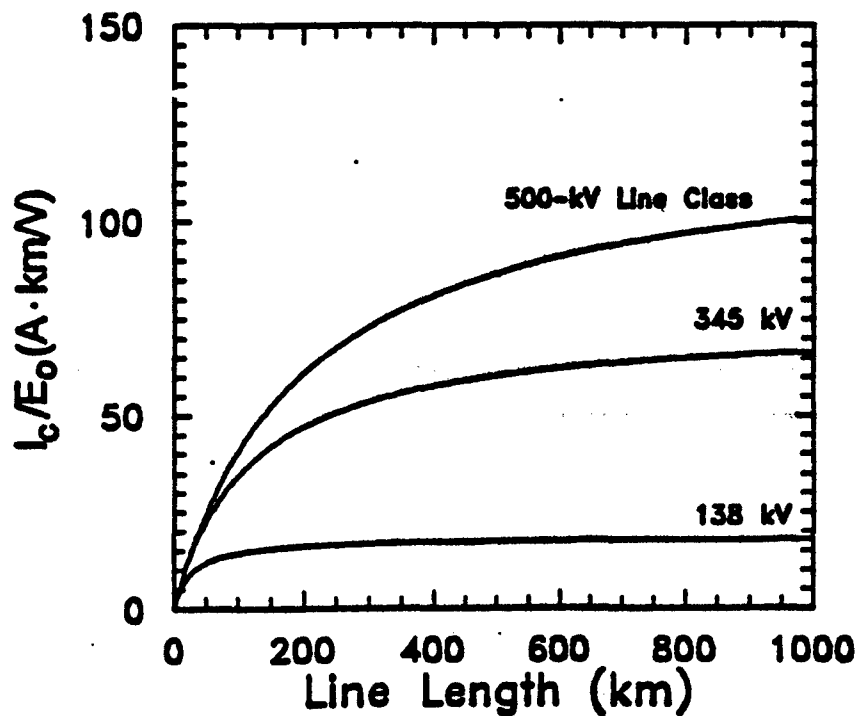


Figure 3-7. MHD-EMP-induced current in transmission lines.

Table 3-1. Maximum normalized MHD-EMP-induced current

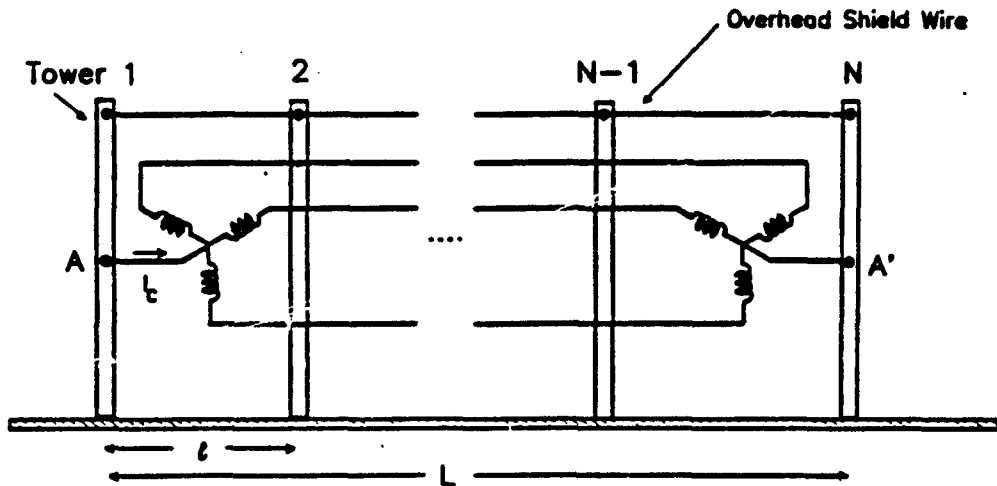
Voltage Class (kV)	I_c/E_0 (A-km/V)
500	120.5
345	74.1
138	18.5
69	16.1
34	13.8
25	13.8
12	11.0

3.5.2 Considerations for Shielded Three-Phase Power Lines.

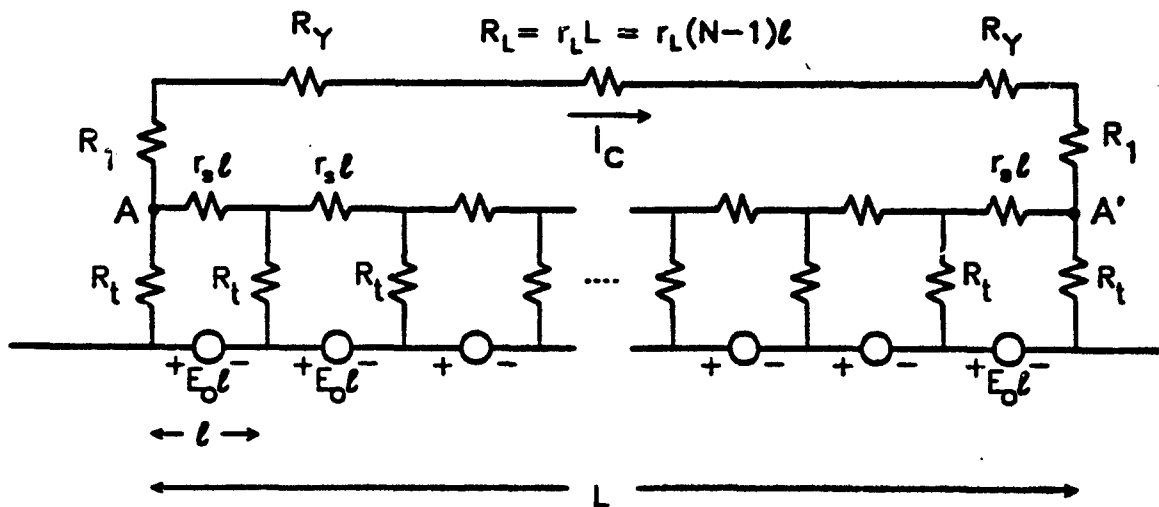
A frequent practice with long transmission lines is to provide one or more overhead shield conductors for lightning protection. Typically, these conductors are smaller than the power phase conductors; consequently, they have a larger per-unit-length resistance. These conductors are grounded at each tower, providing a conducting path to local ground. The MHD-EMP earth-induced E-field can also induce currents in these shield wires, and if the three-phase power system is connected in some manner to the shield system, these currents can influence the level of current flowing in the transformer neutrals.

Reference [1] has also considered the E_3 coupling to this type of conductor configuration. Figure 3-8 shows the case of support towers and an overhead shield wire added to the three-phase line previously shown in Figure 3-6. The overall line length L has N support towers, with a distance l between them. The phase conductors are supported by the towers, but do not have electrical connections to them. An overhead shield wire having a per-unit-length resistance of $r_s \Omega/\text{km}$ is connected electrically to the towers, and each tower is assumed to have a grounding resistance through the earth of R_g . The resistances R_y represent the winding resistances of the transformers at each end of the line, and R_l are very small contact resistances of the transformer neutral connections at points A and A'. These latter resistances are usually neglected.

The determination of the MHD-EMP-induced current flowing in the neutral circuit of the transformers I_c is discussed in detail in [1]. This involves developing a Thevenin equivalent circuit for the periodically grounded neutral circuit at locations A-A' in the figure, and then computing the response for I_c analysis using an equation similar to Eq.(3-3).



a. Physical line configuration



b. Electrical circuit model

Figure 3-8. Three-phase line with N towers and overhead shield wires.

To provide an indication of the MHD-EMP responses for shielded power lines, a set of calculations for the 7 different types of transmission and distribution lines (500, 345, 138, 69, 34, 25, and 12 kV classes) has been analyzed in [1]. Each case had line and grounding parameters typical for the voltage class of the line being considered. As an example of a typical calculated response, Figure 3-9 shows the contours of the normalized transformer neutral current I_c/E_0 for various combinations of line length and number of tower sections for a 500 kV class power transmission line. The straight line in this figure represents the locus of points corresponding to the 300 m tower span length typical for this class of line.

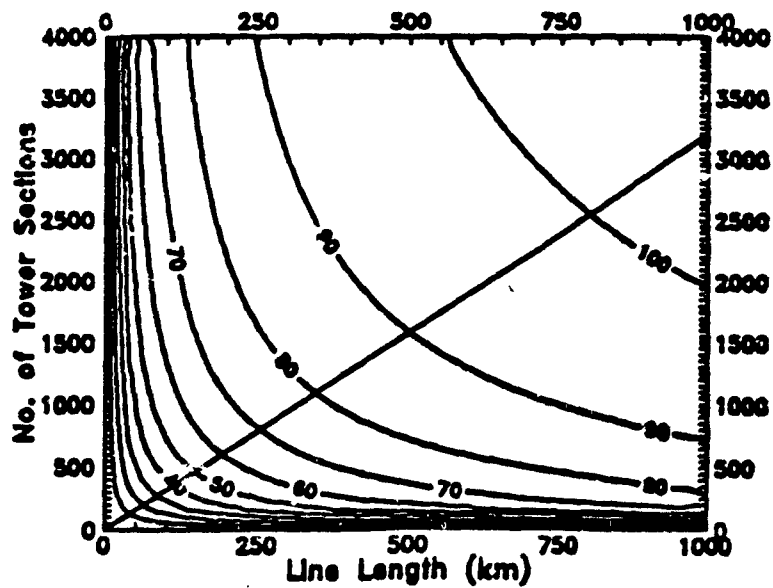


Figure 3-9. Contours of normalized MHD-EMP-induced current I_c/E_0 (A-km/V) for a 500 kV line with grounded shield wires.

3.6 E_3 COUPLING TO A FACILITY WITH LONG LINES ATTACHED.

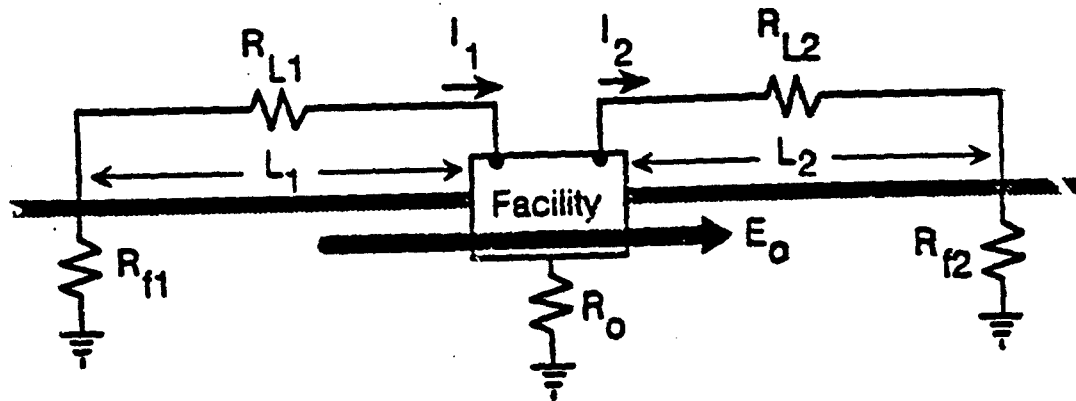
A potentially serious coupling configuration for a buried system is shown in Figure 3-10a, where two long, above-ground conductors are physically connected to a buried facility. The earth-induced E-field E_o is able to cause a current to flow in the long lines and this current is injected directly onto the facility enclosure.

As in the analysis described in the previous sections, each long line is characterized by its per-unit-length resistance r_L , its length L , and a footing resistance R_f at the end of the line opposite the system. The facility itself has a footing resistance R_o which typically will be much smaller than the other resistances in the problem.

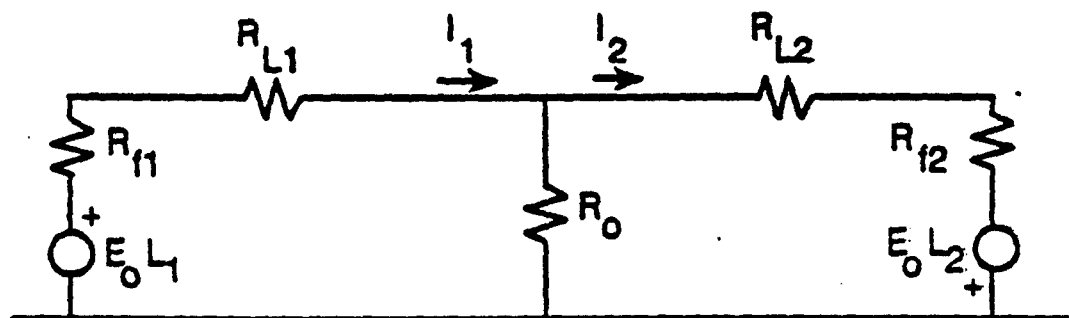
Reference [4] describes an approach to calculate the currents I_1 and I_2 on the wires connected to the facility using the equivalent circuit shown in Figure 3-10b. For this circuit, explicit expressions for the currents flowing onto the facility can be derived and are reported in [4].

The appropriate values of the footing resistance and the per-unit-length line resistance in this model depend on the type of conductor connected to the system. For a 12 kV power system neutral conductor having a typical sub-station footing resistance of $R_f = 0.75 \Omega$ and a line resistance of $r_L = 0.875 \Omega/\text{km}$, ref. [4] shows that the maximum possible induced current is on the order of 11 A for an E_3 environment of 10 V/km.

The E_3 current in this example is limited by the relatively high line resistance which is typical of the 12 kV power system neutral conductors. Larger currents can be expected if the wire is bigger in diameter or if a different line configuration is encountered. For example, ref. [1] calculates a maximum current of approximately 200 A (for a 20 V/km E_3 environment) for a three-phase 12 kV power system with a grounded wye transformer at both ends of the line. If the grounded wye connection is made directly to the system, this current can flow over the system enclosure to ground, and injects an order of magnitude more current excitation on the system.



a. Facility configuration



b. Equivalent circuit

Figure 3-10. Buried facility with direct connection of long lines.

3.7 GROUND CONDUCTOR ISOLATION IN FACILITIES.

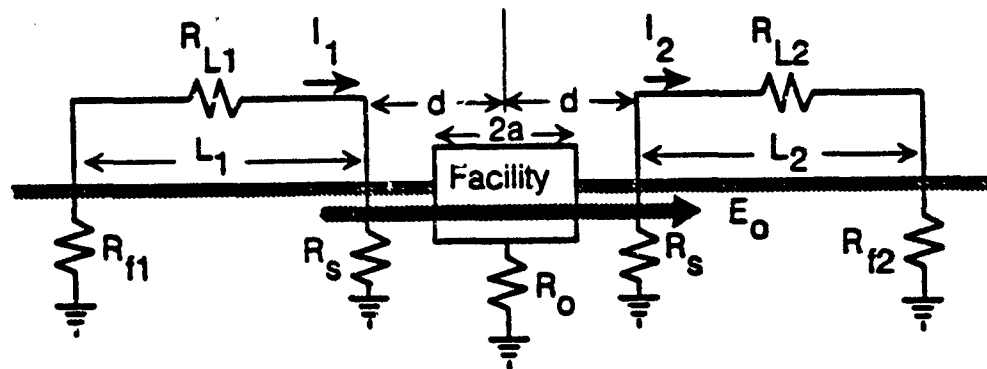
It has been suggested that one way of mitigating the possible effects of the E_3 current on a system is to interrupt the current flow on the system [2]. As shown in Figure 3-11a, this can be accomplished by disconnecting the incoming lines to the facility and grounding them at a distance d from the system. Doing this not only changes the current distribution on the system, as discussed in [4], but it also changes the levels of the injected current due to the introduction of the additional footing resistance R_x of the earth connection.

To calculate the currents I_1 and I_2 , the equivalent circuit of Figure 3-11b has been developed in [4]. This is of the same form as in Figure 3-10b, but with the additional footing resistance R_x . In this case the common resistive element between the two circuit loops R_m is the mutual resistance between the two ground electrodes. As in the previous case, explicit expressions for the current flowing on the lines can be derived. This current, however, generally will be smaller than that for the case when the lines are connected directly to the facility, due to the increased footing resistance, R_x .

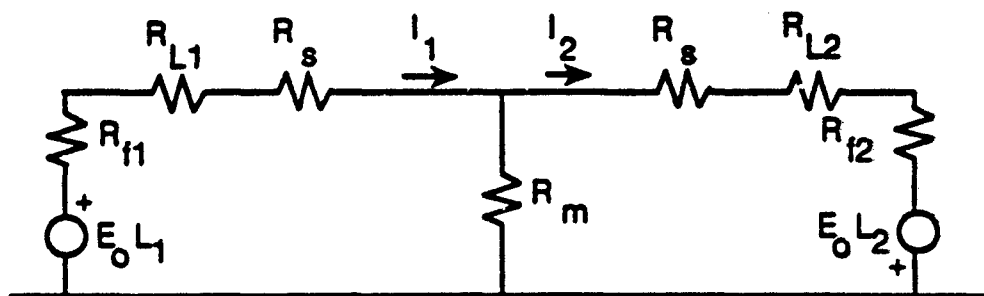
Once the E_3 current flowing in the lines is determined, the fraction of this current collected by the buried facility must be estimated. As described in ref. [4], a possible model for doing this is shown in Figure 3-12. Computing the current density flowing onto the hemisphere from two point electrodes and integrating this as in Eq.(3-2) provides an estimate of the total current collected by the facility.

This integral cannot be evaluated in closed form, but it is easily integrated numerically. Figure 3-13 presents the normalized current flowing into the system I/I_0 as a function of the ratio d/a . As noted in this figure, for a reduction of the total current in the system to 10% of the initial value, the necessary current injection points must be located at $d/a \approx 3.8$, a value which is consistent with $d/a = 4$ of ref. [17].

Thus, the current collected by the facility is reduced by two mechanisms: a decrease in the coupling efficiency of the long lines due to the addition of a grounding resistance of the earth electrode, and the spreading out of the ground currents due to the electrode placement away from the facility. An additional decrease in the magnitude of the E_3 -induced current is expected if the incoming lines are periodically grounded at support towers.



a. Facility configuration



b. Equivalent circuit

Figure 3-11. Buried facility with isolation of long lines.

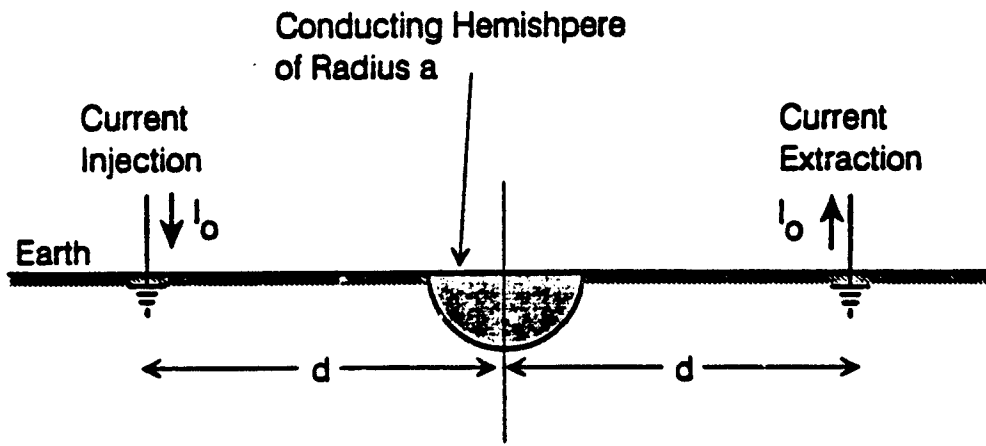


Figure 3-12. Geometry of idealized facility and current injection electrodes.

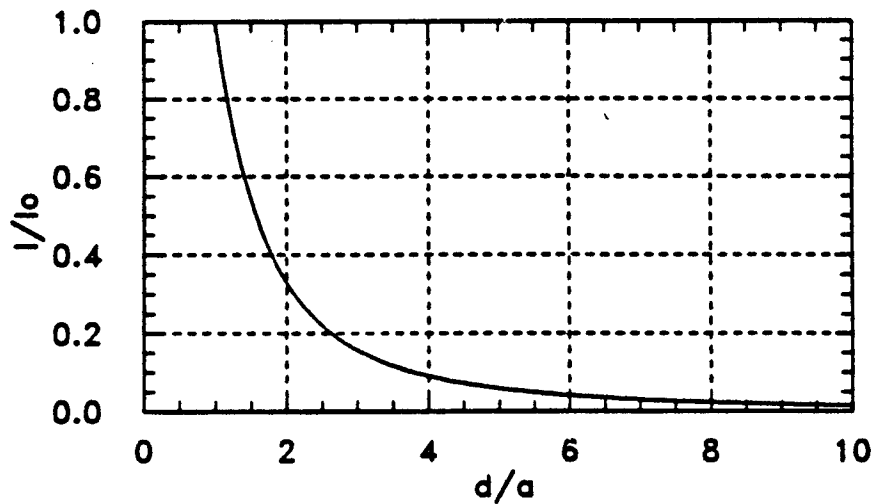


Figure 3-13. Normalized current collected by the system as a function of the electrode positions.

SECTION 4 MHD-EMP TESTING

4.1 OVERVIEW.

During the course of this effort for DNA, several studies related to experimental aspects of MHD-EMP effects on systems have been conducted [4], [7], [18]. These consisted of the development of concepts for MHD-EMP simulation, measurements on a buried communications facility, and laboratory measurements on a mock-up of an electrical power distribution system. This section summarizes these activities and their results.

4.2 MHD-EMP SIMULATION CONCEPTS.

4.2.1 Single Lines.

Because of the quasi-dc nature of the MHD-EMP environment, the most efficient simulation concepts involve injecting a suitable dc current into cables and power lines, or directly onto the exterior of a facility. This is in contrast to the E_1 testing, where it is possible to simulate the incident HEMP fields over the system. Only systems with typical dimensions on the order of several kilometers are strongly affected by the E_3 environment, and it is impossible to excite such large systems with a distributed field source.

There are several different methods proposed for simulating the effects on the E_3 environment on facilities, and the theoretical basis for these simulation methods has been developed in Appendix A of ref. [2]. In that report, the E_3 excitation of long conductors, such as a three-phase power line or a periodically-grounded neutral conductor, has been considered. These types of conducting appendages are viewed as being the most important in collecting the MHD-EMP energy. As discussed in Sec. 3.3, the collection of the E_3 -induced ground currents by a buried facility alone is much smaller than that collected by long lines.

The basic geometry defining the long-conductor excitation by E_3 and the subsequent injection of current into a facility is shown in Figure 4-1. A long conducting line of length L and per-unit length resistance r_L (Ω/m) has a load resistance R_{L1} and an earth grounding (or footing) resistance of R_{g1} at its end far from the facility. At the facility, the line penetrates into the enclosure, where an effective load R_{L2} is present, along with a facility grounding resistance R_g . The response of interest in this case is the current entering the facility I_f .

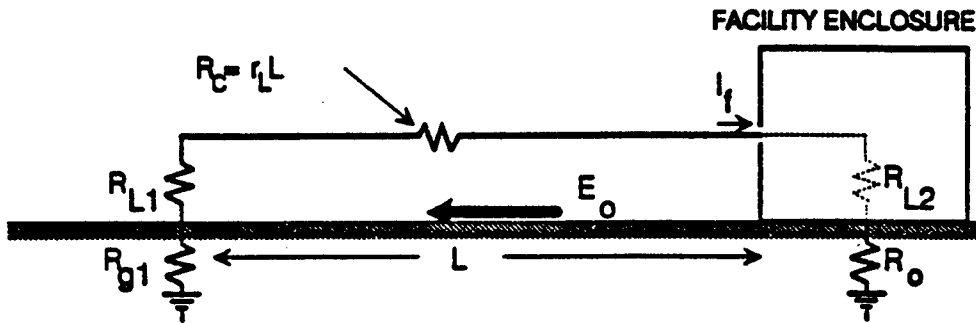


Figure 4-1. An isolated single conductor entering a facility excited by MHD-EMP.

The quasi-static MHD-EMP E-field waveform $E_o(t)$, induced in the earth by the time variations of the geomagnetic field, exists over the entire length of the line, and produces an effective voltage source of $E_o L$ in the line. This voltage source occurs in *series* with the long line. Because of the simple quasi-dc nature of this excitation, Eq.(3-3) can be used to calculate the MHD-EMP-induced current flowing into the facility, with $R_{T1} = (R_{L1} + R_{g1})$ and $R_{T2} = (R_{L2} + R_o)$.

In the simulation concepts discussed in ref. [1], the goal of the simulator source design is to insure that the same quasi-dc current flows into the facility when the E_3 excitation is replaced by the pulser. Figure 4-2 illustrates the replacement of the long conducting appendage of Figure 4-1 by a Thevenin equivalent circuit of the line which is located close to the facility. In this case, both the voltage source V_s and the internal resistance R_s of the source must be adjusted to provide the proper values corresponding to the physical situation. These values are given as

$$V_s = E_o L \quad (4-1)$$

and

$$R_s = R_{L1} + r_L L + (R_{g1} - R_{g2}) , \quad (4-2)$$

where R_{g2} is the grounding resistance of the simulator source shown in Figure 4-2. Because the Thevenin source is connected to the earth at a location different from the original end of the line, this grounding resistance may be different from the original grounding resistance R_{g1} .

As discussed in [1] an alternate, but equivalent, simulation configuration is possible using a Norton short-circuit equivalent circuit. However, as the Thevenin open circuit voltage source is expressed directly in terms of the earth-induced E-field E_0 , the Thevenin equivalent representation of the pulser is the most intuitive of the two. Consequently, nothing more will be said about the Norton source models.

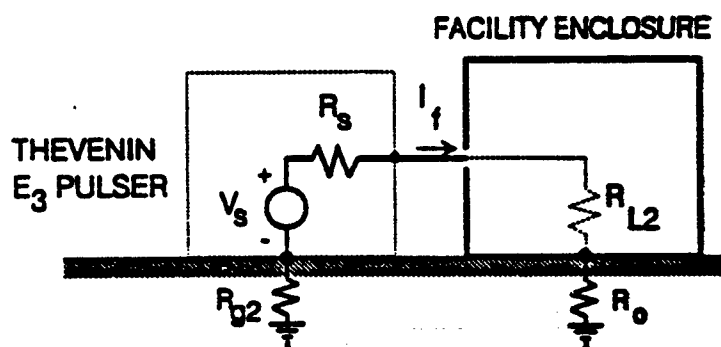


Figure 4-2. Simulation of MHD-EMP excitation by an equivalent Thevenin circuit.

An alternate simulation configuration for long lines is suggested in [1]. In this case, the line is left intact, and the E_3 source (or "pulser") is inserted in series with the line, as shown in Figure 4-3. The line load, footing, and conductor resistances are all unchanged, and if the line normally carries communications signals or electrical power, it can continue to operate normally as the E_3 signals are applied. The Thevenin source impedance R_s should be chosen to be much smaller than the sum of all of the other resistances in the circuit, and the voltage source is given by Eq.(4-1). In this event, the facility current will be correctly simulated.

At times, it may be difficult to insure that the pulser resistance R_s is sufficiently low. In this event, ref. [1] discusses the possibility of increasing the pulser voltage to overcome the effects of this additional resistance.

A third possible simulation configuration discussed in [1] has the E_3 pulser positioned between the line and the ground at a location x_p , as shown in Figure 4-4. This is similar to one of the current injection configurations suggested in MIL-STD-188-125 (ref. [19]). As in the previous case, the normal configuration of the long line is left intact, so that the E_3 pulser need not simulate the normally-occurring signals or power on this line. However, the presence of the pulser will tend to short out a portion of the signal or power at its location x_p .

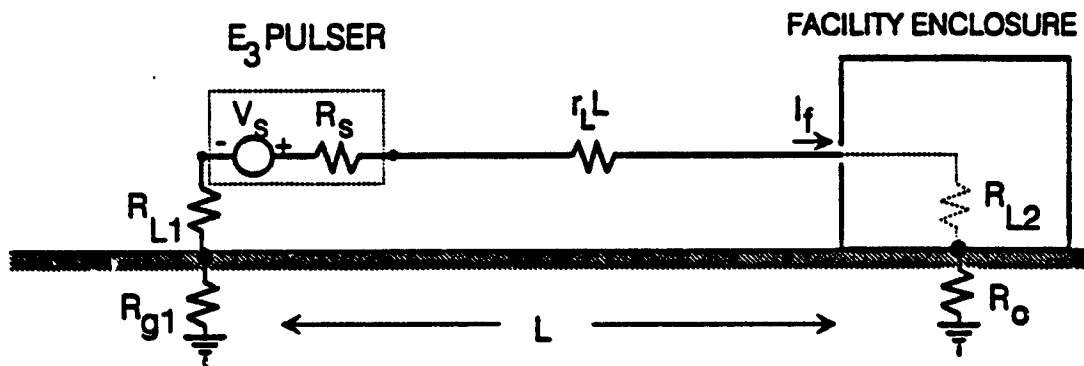


Figure 4-3. MHD-EMP simulation with the pulser in series with the line.

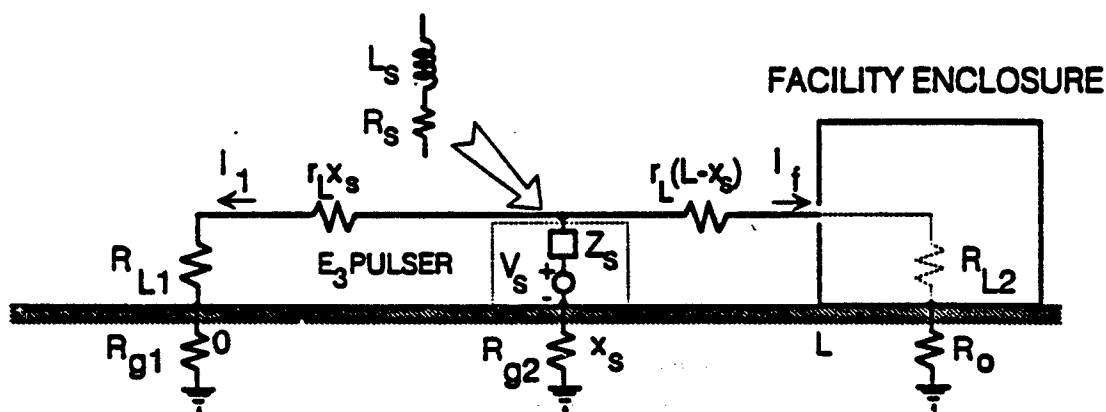


Figure 4-4. MHD-EMP simulation with the pulser across the line.

To minimize this loading that the pulser has on the system, the pulser impedance should be large at the power or signal frequency. This can be achieved by constructing the pulser impedance as a series $R-L$ circuit, so that $Z_s = R_s + j\omega L_s$. The inductance L_s is chosen such that $\omega L_s \gg R_{L1} + R_{g1}$ or $R_{L2} + R_o$. In this way, the pulser can inject an E_3 signal into the system, but the normal operation of the system is not adversely affected.

Although it is possible to inject a current into the facility in this manner, this source configuration does not correspond to that arising from MHD-EMP excitation in which the source is located in series with the line. This difference in the source configuration can give rise to response modes that are not present under E_3 excitation. For example, under an actual MHD-EMP excitation, the currents I_I and I_f in Figure 4-4 are expected to be identical, both in magnitude and direction of flow. This will not necessarily be true, however, if the pulser is shunted across the line, as shown in the figure.

The possible differences in the currents I_I and I_f may not be important in all instances. If the only concern is in providing the proper quasi-dc current to the facility, the simulation with a shunt pulser may be adequate. However if the interaction of the E_3 -induced currents on the line with the load R_{L1} is important (possibly due to the presence of saturatable magnetic material in the load), this simulation concept is not optimum. This becomes particularly important in power system simulation, as mentioned in [1].

Other configurations of long lines have been considered. Figure 4-5 illustrates a periodically-grounded line, such as the neutral or shield conductor of a power line. For typical parameters of a power line, the effects of the periodic grounds have been seen to reduce the injected current into the facility by about 30% [1]. Simulation concepts for this line are also discussed in this reference.

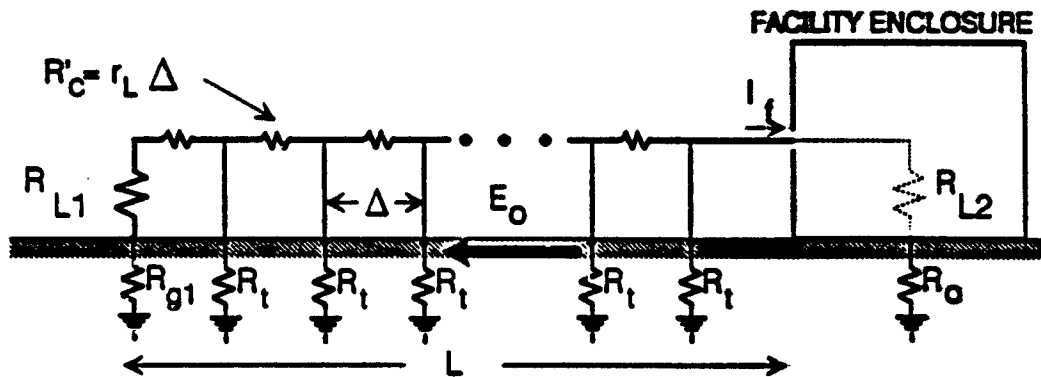


Figure 4-5. Configuration of a single line periodically connected to earth.

4.2.2 Three-Phase Power Lines.

Due to their long lengths, three phase ac power lines entering the facility are potentially important collectors of MHD-EMP energy. In contrast with most single penetrating conductors discussed in the previous section, the three-phase conductors carry normal 60 Hz power, and the MHD-EMP-induced currents on the line can interact with the energized power equipment to saturate transformers. This saturation creates harmonics within the system, and unless the testing is performed with energized equipment, the effects of these harmonics cannot be fully determined. The requirement for performing E_3 simulations on energized power equipment poses many problems, including personnel and equipment safety, and the desirability of not interrupting the normal operation of the facility or the commercial power network. As in the case of the single conductor penetration into the facility, there are a number of different E_3 simulator configurations that are possible for the case of three-phase penetrations. These also have been discussed in detail in ref. [1].

A possible line configuration for supplying ac power to a facility is the three-phase line shown in Figure 4-6. A simple version of this line consists of three parallel conductors of length L , each having a per-unit-length resistance of r_L (Ω/km). At the end of the line distant from the facility, the line is terminated in a grounded wye transformer secondary having winding resistances R_y for each phase, a neutral conductor resistance R_{LN} , and a grounding resistance R_g . Normally, these transformers are balanced so that the resistances in each phase are identical. In this example, no neutral conductor is carried with the phase conductors. Different electrical utilities have different practices for constructing transmission and distribution lines, and this case is typical of some lines in California. In other instances, a fourth neutral line might be carried with the phase conductors.

For this configuration, the primary of the transformer is connected to other parts of the electrical power network, and this supplies the normal 60-Hz power to the line and the facility. Although this power source is not explicitly indicated in Figure 4-6, it could be represented by three 60 Hz voltage sources in series with the transformer secondary resistances R_y . In addition to these normal operating voltages, there is the earth-induced E-field caused by the MHD-EMP.

Several different simulation concepts for this line configuration have been developed in [1]. Figure 4-7 illustrates the most general concept, which replaces the excited line with a generalized Thevenin circuit, similar to that in Figure 4-2 for the single line. In this case, the

individual resistances in the wye circuit are R_y and consist of the series combination of the transformer winding resistances and the phase conductor resistances. The other pulser resistance R_{s_j} takes into account the possible difference in grounding resistance at the pulser location. These quantities, as well as the voltage sources, V_p , are discussed in the reference.

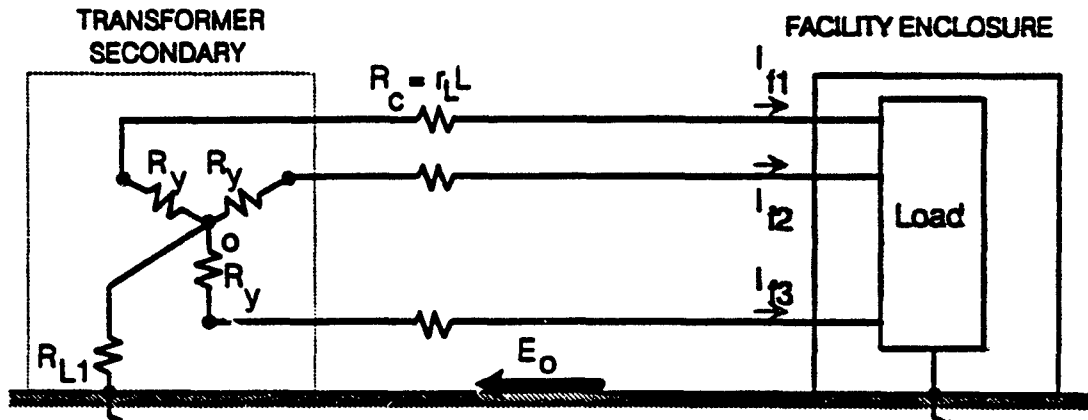


Figure 4-6. E_3 excitation of a three-phase power line.

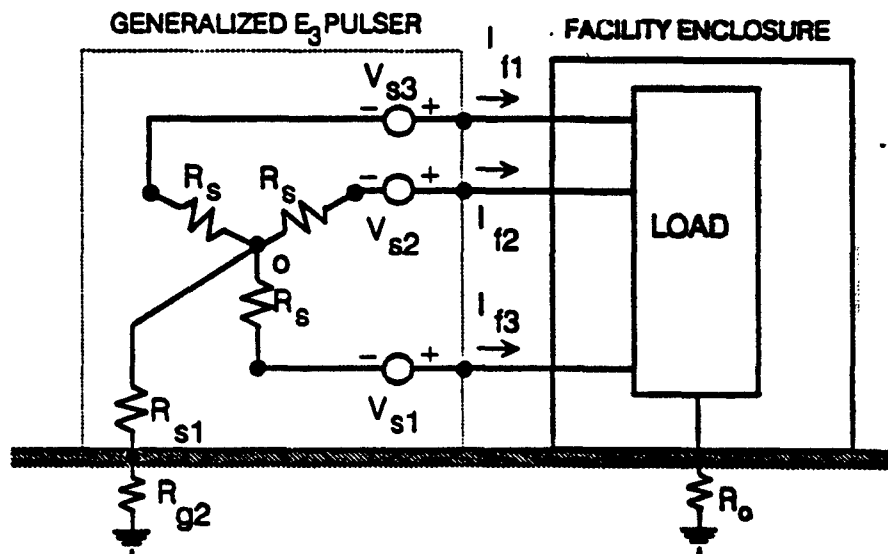


Figure 4-7. Thevenin equivalent circuit excitation of a three-phase line.

An alternate simulation procedure is shown in Figure 4-8, in which the three-phase line is left intact and the quasi-dc MHD-EMP voltage is injected through the neutral of the grounded wye transformer. In this manner the normal operation of the transformer continues during the simulation, and the 60-Hz power remains on the lines without additional sources. In addition, the normal saturation characteristics of both the wye transformer and possibly of the internal facility loads will automatically be included in the simulation. If the internal load grounding connection is a well-defined, single-point ground, as shown in the figure, the E_3 pulser could be located at point A in the figure, instead of at the end of the line. This might be desirable if the line is very long.

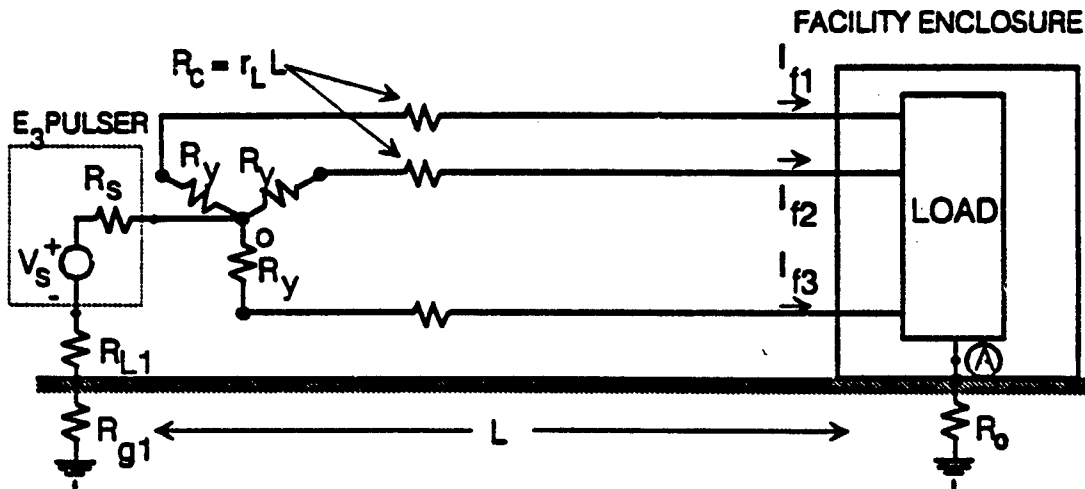


Figure 4-8. E_3 simulation of a three-phase line with pulser in the transformer neutral conductor.

It is also possible to consider locating the E_3 pulser along the line at a location x_s . Figure 4-9 shows a pulser consisting of three voltage sources and resistance elements. This case is similar to the single-line simulation shown in Figure 4-4. As in the previous single wire case, the goal here is to choose the voltage sources in such a way that the quasi-dc current entering the facility is the same as in the case of MHD-EMP excitation. In addition, there is a requirement that the presence of the pulser should not significantly affect the normal operation of the power line. Thus, the source resistances R_s in Figure 4-9 should be large compared with the normal resistances of the line.

An analysis of the currents flowing into the facility in Figure 4-9 can be performed by using the dc models developed in [1], and this can lead to explicit expressions for the voltage sources V_s in terms of the E_3 -field and line properties. This simulation configuration is not particularly recommended, however, because it is important to insure that both the source transformer and the load circuit have the proper simulated excitation. This is particularly critical if the effect of the 60-Hz harmonics generated within the system is to be monitored. In the present simulation concept, there is no guarantee that these harmonics will be generated properly, for the current flowing into the source transformer is considerably different from that experienced with the actual MHD-EMP excitation.

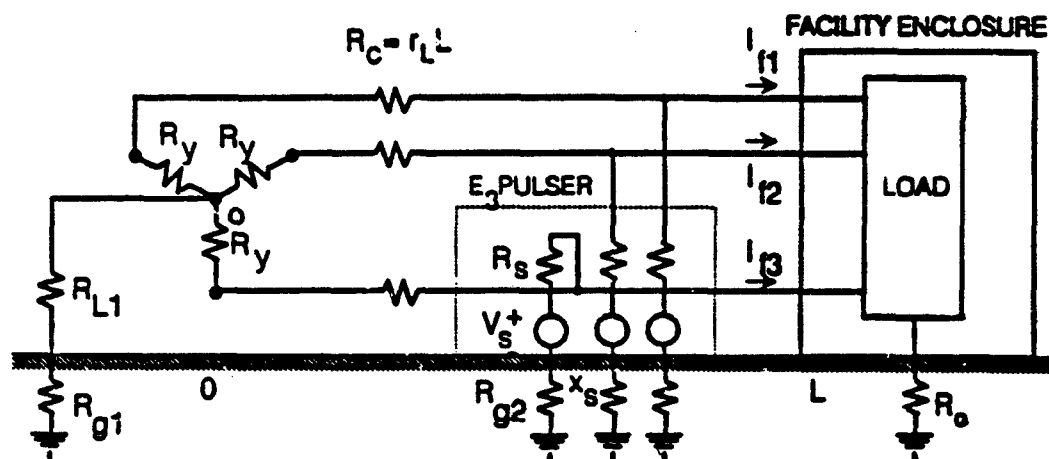


Figure 4-9. E_3 simulation of a three-phase line with pulser along the line.

The addition of a fourth neutral conductor to the three-phase line of Figure 4-8 complicates the simulation procedure. This case is discussed in more detail in [1]. As the number of conductors and system complexity increase, the required number of E_3 pulsers also increases. Certain trade-offs regarding to the accuracy of the simulation versus the complexity of the required simulation hardware can be made, and some of these issues are discussed in ref. [1].

4.3 MHD-EMP TESTING ON A BURIED FACILITY.

During the two-week period of May 11-29, 1992, a series of tests on a Federal Emergency Management Agency (FEMA) facility at Olney, MD, was conducted to determine the possible effects of MHD-EMP on ground-based facilities. These tests were part of a larger test program [18] which addressed the responses of this facility to the early-time E_1 and E_2 high-altitude electromagnetic pulse (HEMP) environments. A preliminary report summarizing the E_3 portion of the test and the lessons learned has been written [4], and a formal test report is expected shortly from the test-conduct contractor.

Very few, if any, E_3 tests have been conducted previously on facilities. Consequently, there is little information or experience on conducting such tests. Furthermore, the effects of such testing on power and electronic equipment within the facility are largely unknown. This test program was begun, therefore, with the view of not only trying to learn about how a facility would respond to E_3 , but also to develop techniques and experience for E_3 testing .

There were three stated objectives for the E_3 testing at the Olney site:

- To determine the requirements for a dielectric isolation zone around the facility.
- To evaluate the common-mode blockage of a delta-wye transformer for E_3 pulses, and determine the differential mode transfer function.
- To evaluate the possible effects of transformer saturation and 60 Hz harmonics on facility power conditioning.

This test used the DNA E_3 pulser to inject simulated quasi-dc currents onto selected parts of the Olney facility. Electrical connections between the E_3 pulser and the facility, or electrical components within the facility, were achieved using several hundred feet of power cable. Voltage and current measurements were made within the facility using a recording digitizer. The measured digitized data from the test were transferred to a portable computer and then off-loaded to a floppy disk storage medium for future analysis and plotting. Strip chart plots of the measured responses were also made for inclusion in the test report.

One key aspect of the test was the investigation of the validity of the requirement for a dielectric isolation zone for long lines connected to the earth near the facility. This involved first measuring suitable internal responses within the facility with the E_3 current injection applied directly on the facility enclosure, and then studying the behavior of these responses as one of the current injection electrodes moves away from the facility.

This test was only partially successful, due to the very low amplitudes of the measured internal system responses. With the E_3 pulser connected directly to the facility and injecting about 200 A of quasi-dc current, responses at only two of the internal measurement points could be recorded. Induced currents on the order of 1 to 2 A on the main power transformer neutral and about 0.5 A on the 480 switch-gear neutrals were measured with the E_3 pulser in this configuration. Responses on the other grounding connections were believed to be comparable to the noise level within the system. This current injection onto the facility exterior caused no upset or other problems within the facility.

When the E_3 pulser electrode was moved off of the facility, the pulser could not maintain the injected current levels, due to the increased footing resistance of the electrode connection. As a result, the current drive to the facility dropped by about 85% and no internal responses at all could be measured.

The limited testing at the Olney facility suggests that the requirement for a dielectric isolation zone described in [2] might be overstated. First, the direct injection of 200 A on the system exterior was barely noticed inside the facility and caused no problems. Thus, the requirement in [17] that this current be reduced by 90% appears overly strict in this case. Second, by moving the line connection from the facility to a grounding electrode away from the facility, an increase in the overall circuit resistance can be obtained. This will further limit the E_3 current flow onto the facility. Finally, long lines that can be electrically grounded at the facility will usually also be periodically grounded at support towers along its length. This grounding will further serve to reduce the current injected onto the facility. It must be stressed, however, that these observations are based only on a short test on one facility. Additional studies are required to better understand these issues.

Another type of test was reported in [4] which dealt with transformer responses to the E_3 environment. With the facility being powered by its auxiliary diesel generators, isolation measurements on the unenergized 13.2 kV/480V delta-wye main power transformer for the facility were made. It was found, as expected, that the common-mode rejection of the delta section of the transformer was very large. Differential mode signals were able to penetrate through the transformer to a certain extent, but for the E_3 waveform, these differential responses were exceedingly small and appear to pose no problems to the facility.

A final E_3 test involved the saturation of the energized 13.2 kV/480V delta-wye transformer. This involved injecting a quasi-dc current directly into one phase of the secondary of

the transformer. Although it is impossible to relate this excitation configuration to that which would be found for E_3 excitation, this experiment did provide evidence that the power transformer can be saturated by a MHD-EMP event.

Although this test was short in duration and limited in scope, a number of useful accomplishments were noted. However, since the test involved only a single facility, care should be used in applying these test observations and conclusions to other facilities. Clearly, additional testing is required to increase the confidence in the "lessons learned" from the test. From the results of this E_3 test, the following observations were made:

- An E_3 test on an active facility can be conducted safely, with only a minimal disruption of the normal activities within the facility.
- 200 A of quasi-dc current injected on the exterior of a shielded facility did not affect (i.e., disrupt or damage) internal electrical equipment.
- The requirement that there be an isolation zone of two times the largest facility dimension appears to be too strict for the case of the Olney facility from several standpoints. The requirement that the E_3 current flowing over the facility be reduced by a factor of 10 appears to be far too large, as a direct injection of the simulated E_3 current provided only barely measurable internal responses. In addition, the actual E_3 current flowing from a long line into an earth grounding electrode utilized in an isolation scheme will be reduced from that of the current on the line connected directly to the facility. This is due to the added footing resistance of the electrodes. It is, however, difficult to generalize these observations to all ground-based facilities.
- E_3 signals picked up from the external ground currents and conducted along water and sewer pipes into the facility appear to be negligible. An examination of the utility pipes indicated that they were in direct electrical contact with the facility enclosure, yet no internal responses on such conductors could be measured.
- Externally applied E_3 stress to the system's exterior did not affect the 480/240 V power system.
- Transformers with a delta-grounded wye configuration provide an effective means of blocking common mode excitations from the primary feed circuit.

- The 13.2 kV/480V transformer provided a 10:1 reduction of differential mode transients arising from the E_3 stress injected directly onto the power system.
- A phase-to-neutral current injection in the transformer secondary of the 13.2 kV/480V transformer produced a small amount of transformer saturation. However, this type of excitation is unlike the E_3 excitation expected for a facility or power system. The E_3 excitation of transformers in a facility will be of concern when the high-voltage side (primary) of the transformer has a grounded wye configuration and a dc current can flow from the earth, through the transformer primary, and back to an earth return at a distant substation. In this case, the E_3 pulser should be located in *series* with the ground neutral connection of the transformer. This eliminates the need for pulser isolation circuitry and multiple E_3 pulsers for each phase conductor of the power system.
- The design of future E_3 pulsers for current injection through the earth should be more robust to account for the large ($\sim 50 \Omega$) footing resistance of earth electrodes.

4.4 MHD-EMP TESTING ON POWER DISTRIBUTION TRANSFORMERS.

In June of 1990, an experimental program was conducted at the Mission Research Corporation (MRC) in Albuquerque, NM, in order to understand the behavior of distribution-class transformers subjected to quasi-dc current excitation [3]. For this experimental program, ORNL was the lead organization, with assistance being provided by ORNL subcontractors, MRC, and the Public Service Company of New Mexico.

This test involved constructing a mock-up of a simple three-phase 12.47 kV distribution system using two distribution-class transformers and a dummy three-phase load bank, as shown in Figure 4-10. This system was fed by local commercial power. Measurements on this system were made with the following specific objectives in mind:

1. To determine the effect of quasi-dc currents on the operation of three-phase transformer banks.
2. To measure voltage and current harmonics within the system and at the loads.
3. To assess the importance of the quasi-dc current duration.

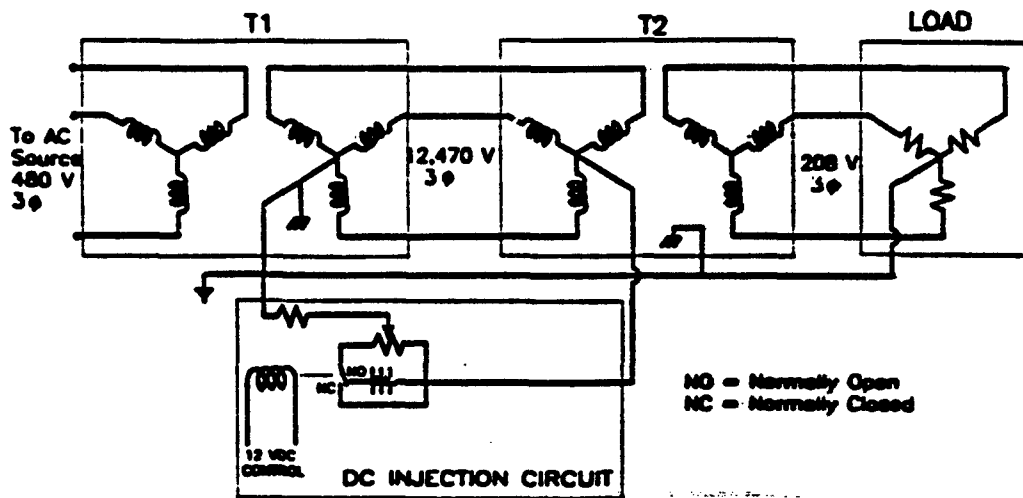
4. To determine the change in reactive power demand as a function of quasi-dc currents.
5. To determine if low level quasi-dc currents and the distorted ac current can cause primary fuses to blow.

Objectives 1, 2 and 4 were determined directly from the data taken in these measurements, while objectives 3 and 5 are determined from interpretations of the data. Given the knowledge of the MHD-EMP-induced current flowing in a long power line, and the transformer response characteristics measured in this test, it is possible to make estimates of the behavior of the electrical power distribution system to the E_3 environment.

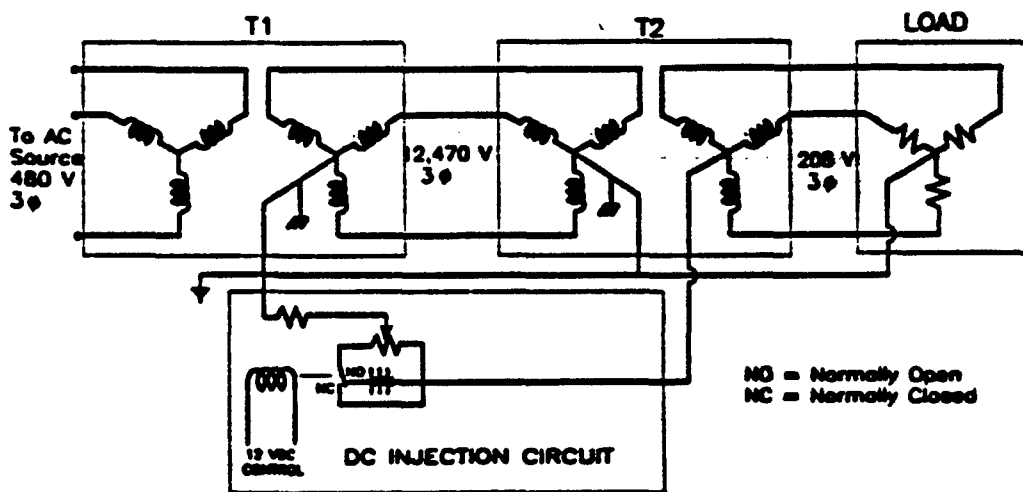
The main part of the data acquisition system for this test involved 12 simultaneous voltage and current measurements on the phase conductors of the system using a digital strip chart recorder which was controlled by a desk-top computer. The quantities measured were the line-neutral voltages on the 12.47 kV side of transformer T2, the corresponding phase currents on two of these high voltage lines, the line-neutral voltages and currents on the three phase conductors on the output (load) side of T2, and the transformer neutral current. The measurement equipment configuration is shown in Figure 4-11.

For each test, the input voltage, current and power were also monitored by a power meter, which provided readings of these quantities on a data tape. These quantities served as a check of the overall operation of the system, and provided an additional means of correcting the V and I measurements on the high voltage portion of the lines so as to insure that a power balance is achieved.

As an example of measured results, Figure 4-12 presents typical line currents on the 12.47 kV primary sections of transformer T2 for configuration 1a. Case "a" shows the normal phase current with no dc current injection into the neutral, and exhibits a reasonably clean 60 Hz sinusoidal waveform. Case "b", on the other hand, illustrates a highly perturbed waveform, arising from the saturation of the transformer cores due to about 5.5 A dc current injection into the transformer neutral.



a. Test configuration 1A



b. Test configuration 1B

Figure 4-10. Transformer test configurations.

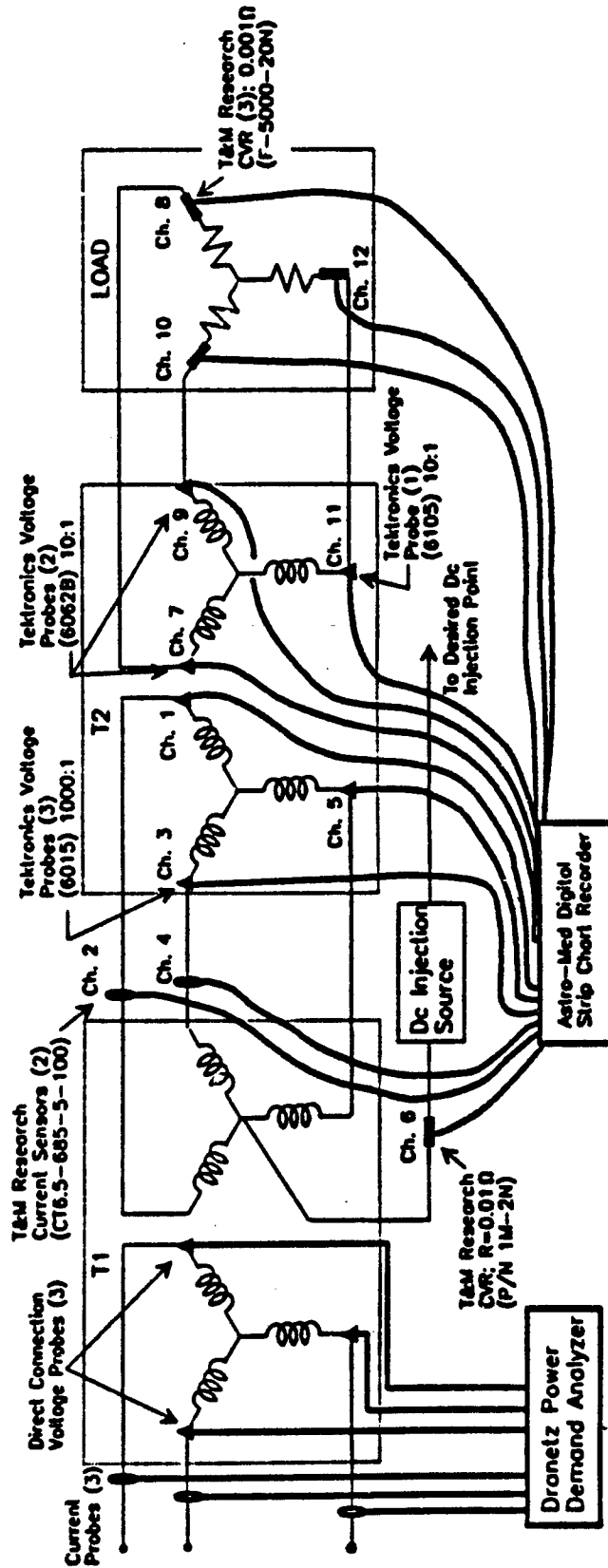
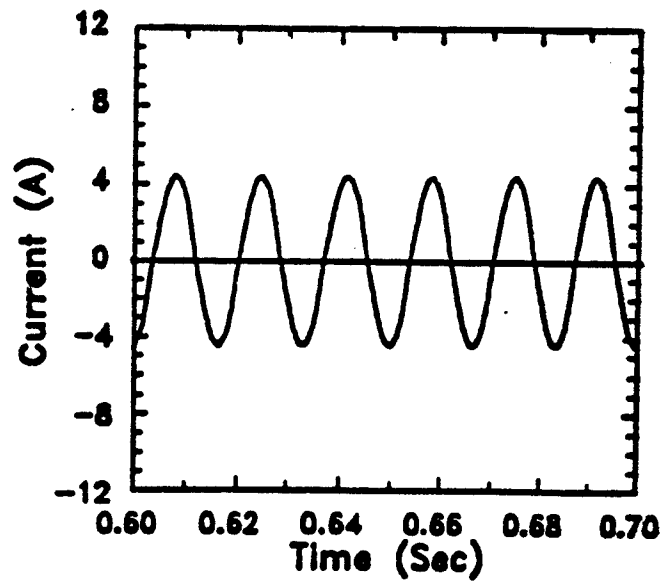
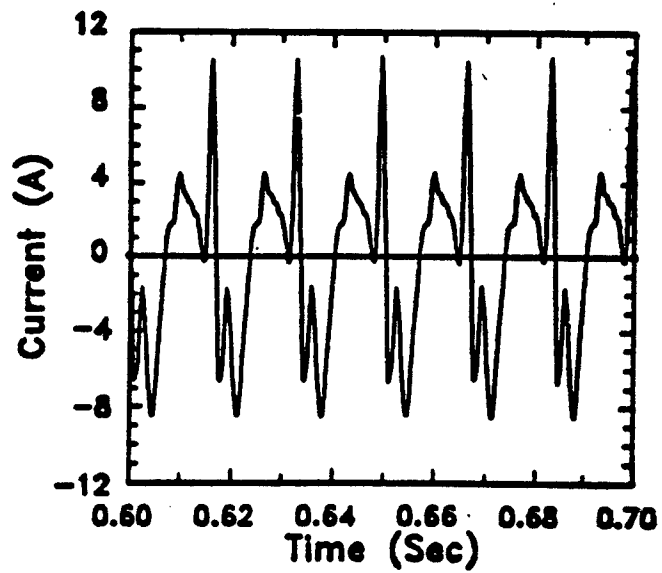


Figure 4-11. Diagram of the measurement set up.



a. No dc excitation



b. 5.5 A dc excitation

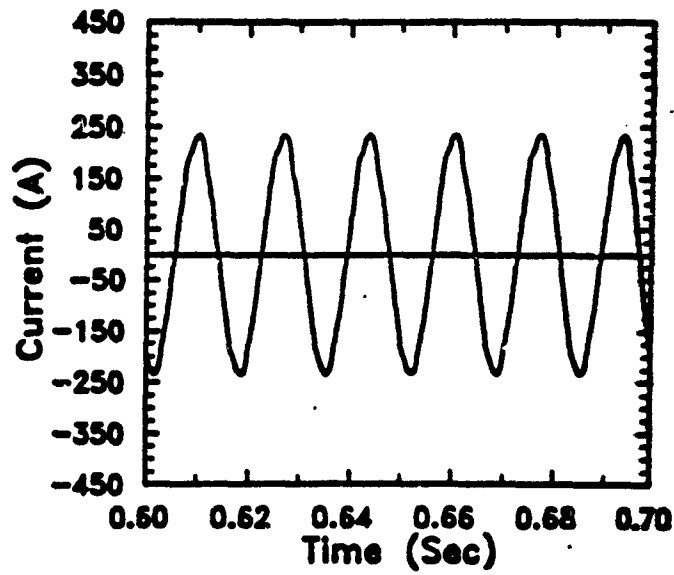
Figure 4-12. Measured current on the primary of transformer T2 for configuration 1A.

Figure 4-13 shows the corresponding results for the phase currents on the secondary 208 V side of the grounded wye transformer. Clearly the harmonics pass directly through the transformer without significant attenuation.

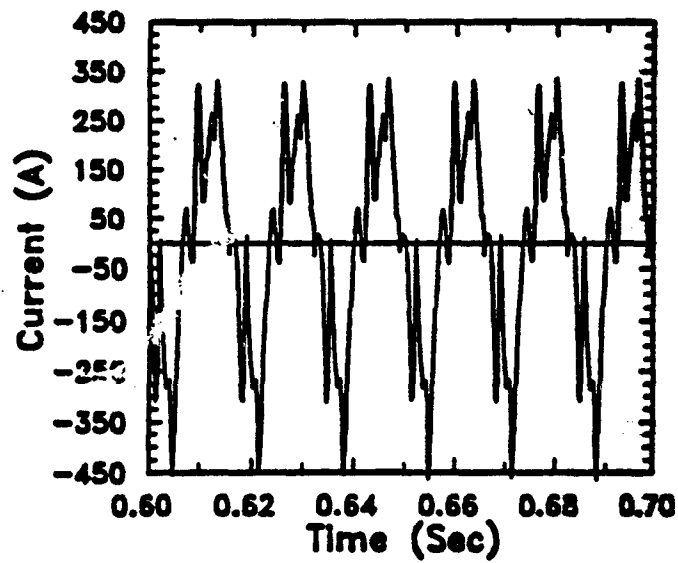
These high harmonics in the transformer current might cause serious problems to the power system. Figure 4-14 shows the Fourier spectra of the transient line currents of Figure 4-12. It is obvious that the higher harmonics of the 60 Hz power frequency are enhanced by this dc current injection. A summary of the harmonic distortion caused in this system is shown in Figure 4-15 in the form of a bar chart. This shows the second (i.e., 120 Hz) and higher harmonics contained in the current in the primary of transformer T2 as a function of the dc current injection level.

One effect of a large harmonic content in the line current is in an increased reactive power demand that is placed on the power generation equipment. Figure 4-16 illustrates the measured increase in reactive power fed into the transformer system, shown as a function of the dc current injection. This is shown for both small and large values of dc current injection. For the injection of dc currents below about 0.1 amps, the transformer continues to operate more or less linearly, with no increase in the reactive power demand. However for currents above this value, the reactive power demand is seen to be a linear function of the injected dc current level.

An additional quantity of interest is the relaxation time which is characteristic of the transformer/load system. Normally this is a function of the dynamic transformer inductance and resistance, as well as the load resistance values, and can have values on the order of many seconds. This quantity was indirectly measured from the changes in the envelopes of the transformer currents as the dc excitation was switched on and off. Figure 4-17 shows an envelope curve of the 60 Hz current flowing into T2 as the dc injection is turned off and then turned on again. In this figure, the finite time that it takes the system to change its state is evident. As might be expected, this system relaxation time is a nonlinear function of the dc injection levels. Figure 4-18 presents the observed system relaxation time as a function of the dc injection. This figure indicates that the injected dc causes the system to react more rapidly than would be expected in the case of no dc excitation of the transformer neutrals. For currents typical of an MHD-EMP excited line (about 100 A), it is expected that the transformers in this system will saturate in times less than 0.5 seconds.

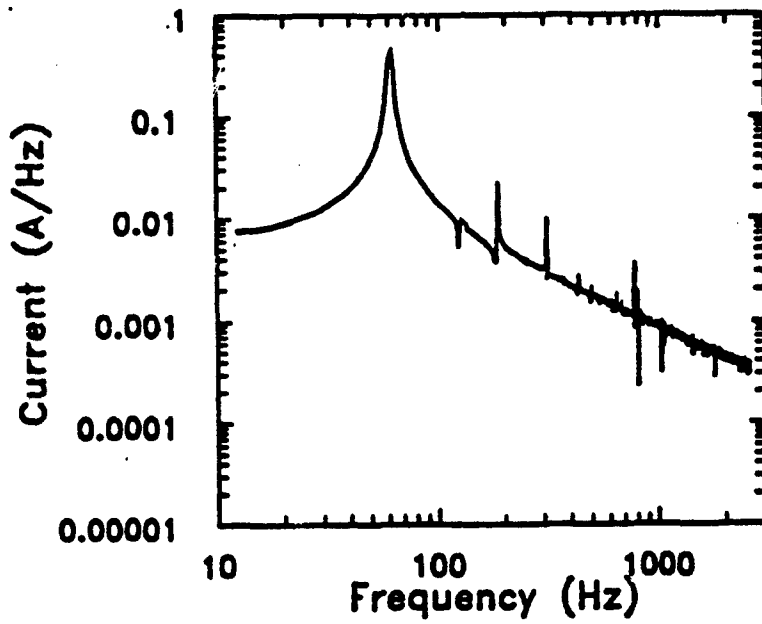


a. No dc excitation

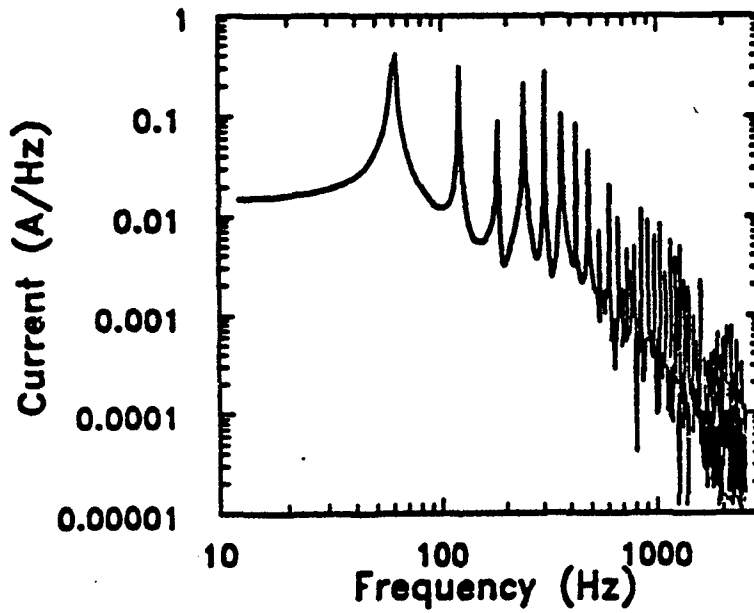


b. 5.5 A dc excitation

Figure 4-13. Measured current on the secondary of transformer T2 for configuration 1A.



a. No dc excitation



b. 5.5 A dc excitation

Figure 4-14. Examples of computed spectra for the measured responses of Figure 4-12.

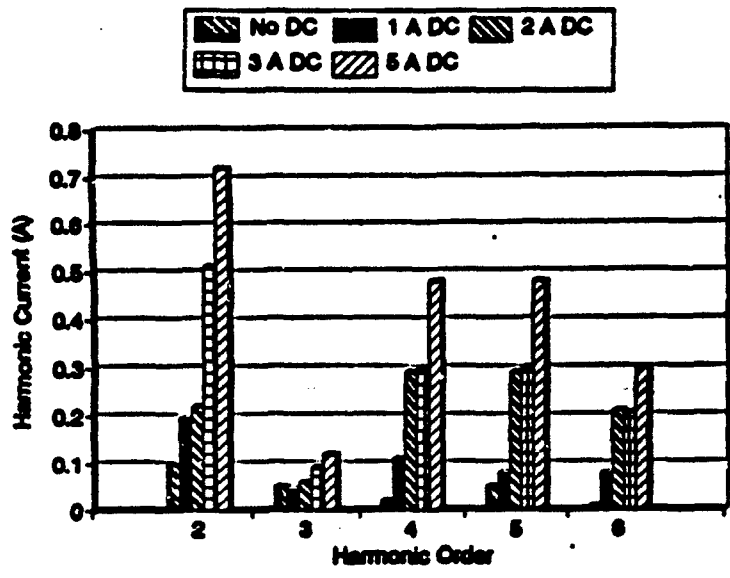


Figure 4-15. Measured harmonic content in primary of T2 for configuration 1A with different levels of dc injection.

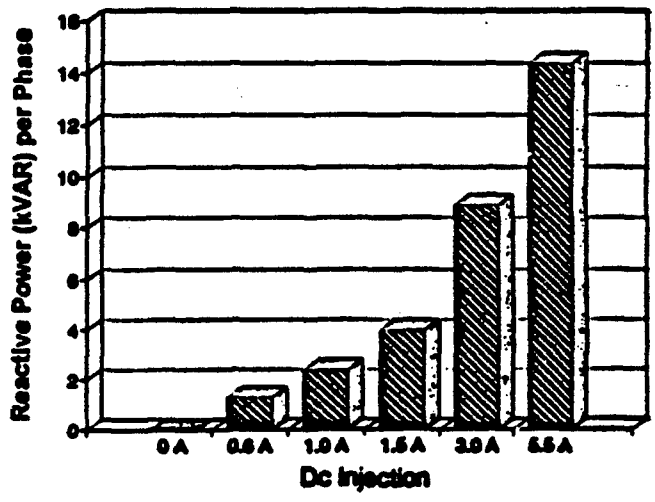


Figure 4-16. Measured reactive power demand.

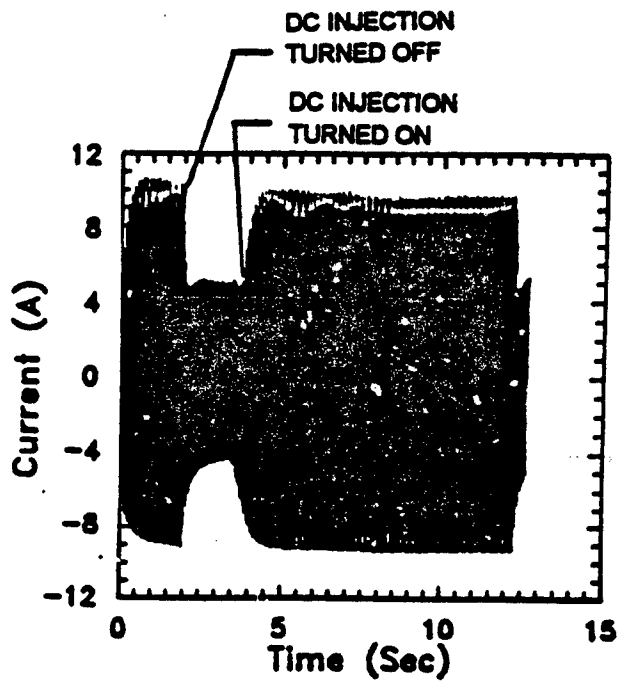


Figure 4-17. Envelope curve of 60 Hz phase current for configuration 1A.

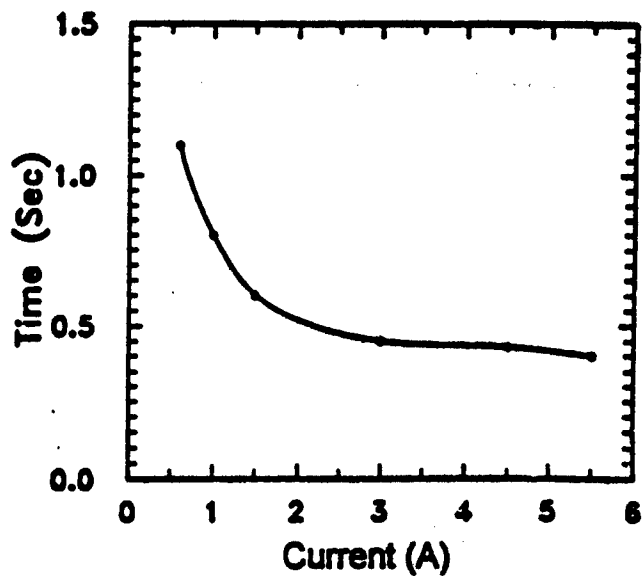


Figure 4-18. System relaxation time.

The measurements made during this experiment answered most of the objectives of the test. If the dc injection is limited to the primary side of the transformer, the majority of the effects are seen in the primary circuit. However, the harmonic distortion at lower order harmonics will be passed through the grounded wye primary to the secondary with potentially adverse effects on the connected load. A delta connected transformer will reduce the harmonics that are passed from the primary circuit to the secondary, since it will not pass common mode harmonics. However, differential mode harmonics, known in the power system community as positive and negative sequence harmonics, will pass through the delta winding transformer.

In addition, this test showed that with sufficient dc injection, the generator supplying the transformers is subjected to a very high reactive power demand. The possibility that the added reactive power load would result in the blowing of fuses on the primary circuit appears to be a real concern.

Transformer damage is very dependent on the dc injection level and duration and the core's magnetic history and thermal performance. During this experiment there was no apparent damage to the test transformers from the series of multiple, 10-15 second tests at various dc injection levels. The thermal mass of coolant in the test transformer was so large that several minutes of injection at saturation level would have been required to have caused physical damage; hence, there would no expected damage during a 10 - 15 second test.

SECTION 5 MHD-EMP MITIGATION METHODS

5.1 GENERAL CONSIDERATIONS.

The protection of ground-based facilities against the effects of MHD-EMP uses measures that are different from those used for protecting against the early-time E_1 HEMP. This is due, in part, to the very low frequency content of the E_3 environment. At sub-Hertz frequencies, a shielded facility becomes more or less transparent to the current induced on its exterior. The applied MHD-EMP current will divide according to the various dc resistance paths within the system, and a portion may flow into the interior. Thus, the global shielding concept that is commonly used for the E_1 hardening is not strictly applicable for the E_3 environment.

An additional important factor to be noted for the E_3 protection is the fact that a large charge transfer is involved in the MHD-EMP current (on the order of 29 kilocoulombs— about 100 times that of a severe lightning flash). Moreover, this occurs with modest open-circuit voltages (only a few kV). It is feasible to consider interrupting the MHD-EMP current and holding off the open-circuit voltages. Such a current interruption has the decided advantage that it can eliminate the shield and filter transparency problems and the high-charge-transfer, low-voltage surge arrester requirements. Furthermore, current interruption can often be achieved with existing equipment, such as power transformers.

References [2] and [6] discuss various MHD-EMP mitigation methods that are available. This section will briefly review these techniques. Generally, to mitigate the effects of MHD-EMP on a facility, all long conductors must be isolated from the building and the commercial power harmonics and voltage swings must be controlled. A power transfer switch within the facility would be expected to respond to the voltage fluctuations as long as the harmonics have not interfered with the switch control circuitry. The major sources of MHD-EMP induced currents are the commercial power lines and neutral conductors; the neutral current indirectly coupling to the facility power or ground system via external current collectors; metal water pipes; phone lines; and other long conductors that enter or come near the facility. Grounded-wye/grounded-wye facility power transformers with the ground connected to both the utility neutral and facility ground will permit a portion of the MHD-EMP current to enter the facility. The major source of harmonics can be the commercial power system.

5.2 MITIGATION TECHNIQUES FOR COMMERCIAL POWER.

The power distribution line serving a facility is expected to be a principal source of MHD-EMP-induced current. The power transformer neutral and neutral conductor are typically grounded at the distribution substation, which may be tens of kilometers away. If they are also grounded to the facility shield, a path into the facility via the facility ground is established. However, if the distribution neutral is terminated some distance away from the facility and a delta-connected primary is used for the distribution transformer serving the site, the MHD-EMP current can be interrupted. This scheme is illustrated in Figure 5-1. The delta-connected transformer primary is an open circuit to the common-mode MHD-EMP current on the distribution system is perfectly balanced, the MHD-EMP current will be completely blocked by the delta primary windings. The delta-connected primary will also reduce, but not completely eliminate, the power frequency harmonics that enter the facility from the power network.

Even if the system is not perfectly balanced, the transformer does not pass the quasi-dc differential-mode (line-to-line) current through to the secondary circuits. The MHD-EMP is still blocked out of the facility, although the line-to-line current in the delta primary may generate 60 Hz harmonics in the transformers that are coupled through the transformer to the secondary circuits. However, the delta winding will provide some protection against harmonic distortion generated elsewhere in the distribution system, since it will not pass zero-sequence harmonics. Other harmonic protection measures are discussed later in this section.

To estimate the separation needed between the facility and the point where the distribution neutral is grounded, ref. [17] analyzed the current flowing into a conducting hemisphere immersed in earth, as shown in Figure 3-12 of the present report. To limit the current through the sphere to 10 percent of the total injected current, the distance to the injection points must be about four times the radius of the sphere. This was used to estimate the separation between long lines and the facility shield illustrated in Figure 5-1. Taking the largest dimension of the shield to be $2a$ (the shield is viewed as a conducting sphere of radius a), the neutral and other long conductors must be grounded a distance $d = 4a$ from the facility to limit the shield current to 10 percent of the MHD-EMP current. This result was used to develop the protection guidelines described in ref. [6].

The recent measurements at the Olney, MD, FEMA facility have cast some doubt on the necessity of requiring this isolation of the neutral conductor. According to a more detailed

analysis of this current reduction scheme in [4], it was found that the overall current reduction is strongly dependent on the grounding resistance and the length of the line. Thus, no single value can be provided for the required conductor isolation, although, for standardization purposes, a single value is preferred. Reference [4] illustrates the required normalized isolation distance d/a for different combinations of line length and resistance parameters. Values range from $d/a \approx 4$ to $d/a = 1$ (i.e., in almost direct contact), depending of the parameters of the problem. As the Olney site was not the best facility for evaluating this effect (due to its large shield and few low-resistance internal current paths), this issue cannot be resolved at this time.

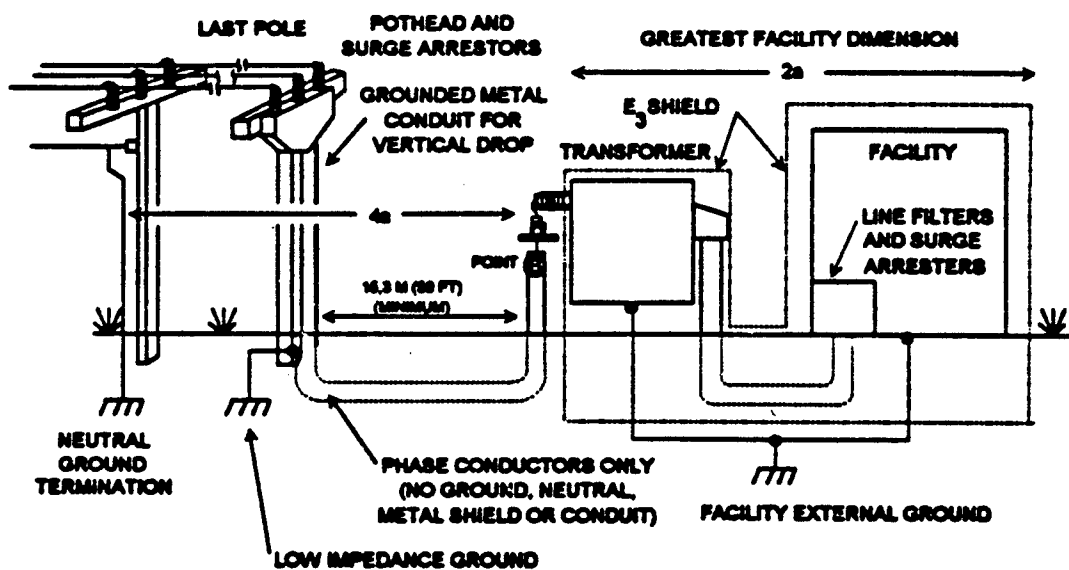


Figure 5-1. Recommended power system design practices for the primary distribution power line configuration.

An issue that deserves additional attention is the requirement that the current collected by the facility must be reduced by a factor of 10 from that occurring if the lines were directly connected to the facility exterior. This requirement was based on the fact that under conditions of a small shield cross-section and a low resistance internal path, the internal magnetic fields might be large enough to erase plated-wire memories in internal facility equipment. Before this requirement is codified into a protection standard, additional work should be undertaken to better define this requirement. In the E_3 test conducted at the Olney

facility, a quasi-dc current of 200 A was directly injected onto the system enclosure and internal current responses were measured to be only a few amperes [4]. No system upset or failures were reported. However, as previously mentioned, the Olney facility may have not been optimal for observing such effects, due to its physical and electrical configuration.

Furthermore, in the Olney test when the current injection electrode was moved from the system to a point a few meters away and connected to the earth by a long electrode, the injected current dropped to about 30 A. For this case, no internal responses could be noted. This marked drop in the injected current level illustrates the effect that the increase in grounding resistance has on the E_3 current, and suggests that real facilities may have an injected E_3 current level that is significantly smaller than a "worst case" current specification. Of course, this condition is not assured in a real system.

Thus, although a requirement for a grounding isolation has been suggested for MHD-EMP mitigation, it is still not clear exactly how strict this requirement should be. It remains an issue to be resolved. However, if a factor of 10 reduction of the external facility current is *assumed* and realistic parameter limits are used, the isolation requirement can be substantially reduced. The grounding resistance R_f of a typical ground rod ($a = 0.25$ inches radius, $L = 8$ feet length) is given approximately in [21] as

$$R_f = \frac{\rho}{2\pi L} \ln\left(\frac{2L}{a}\right) \quad (5-1)$$

where ρ is the ground resistivity in $\Omega\text{-m}$. For $\rho = 100 \Omega\text{-m}$, $R_f \approx 43 \Omega$. For larger values of the ground resistivity, the resistance R_f has a larger value. Thus, 43Ω is near the lower limit for grounding resistance of a single rod grounding system.

The other parameter of importance in determining the level of induced MHD-EMP current is the line length. While residential distribution circuits can be on the order of 50 km in length, residential and industrial circuits longer than 30 km are rare. Thus, the E_3 -induced currents on these circuits will probably be much smaller than on the longer transmission lines.

For $R_f = 43 \Omega$, a line length $L = 30$ km, and taking into account the reduction in the MHD-EMP induced current due to the multiply grounded neutral (providing a reduction factor of about 15 %), the required d/a ratio can be shown to be on the order of two. Since buried conductors in contact with the soil provide about a factor of ten reduction of MHD-EMP

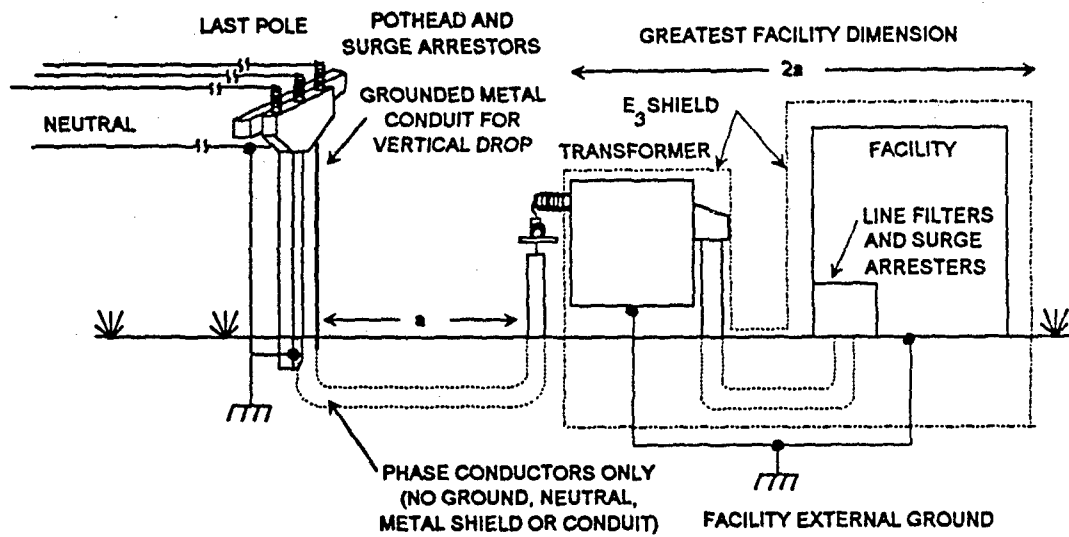
induced current over that in above-ground lined, it is only necessary to isolate metal pipes, etc. from grounded neutrals by the same isolation criterion. Figure 5-2 illustrates a more relaxed isolation requirement.

The isolation of the distribution neutral and the delta connected primary protect the facility from the MHD-EMP. To protect the transformer and underground cable from E_1 , lightning on the power line, and other surges, and the cable terminators at the last pole must be provided with surge arresters connected to a low resistance ground such as a multiple ground rod system. The facility transformer should be protected with MOV surge arresters that do not remain conducting after E_1 and E_2 , so that they are nonconducting during E_3 (this should not be a problem, since the distribution voltage is usually at least a few kV). Figure 5-3 shows the surge arresters at the transformer terminals.

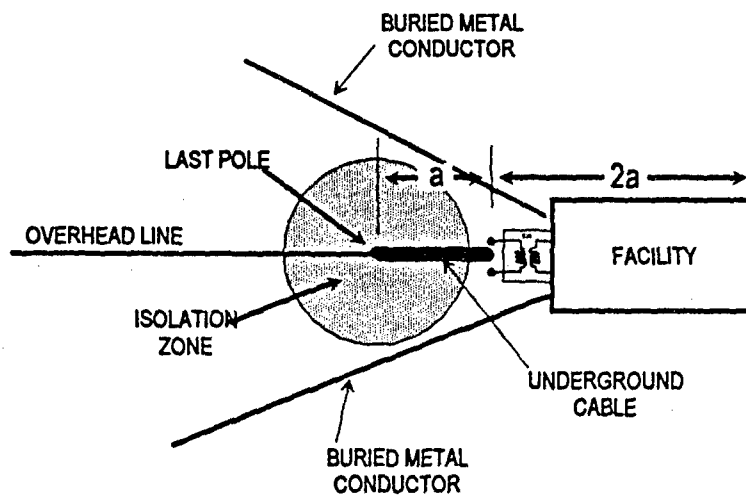
To protect against a fault in the primary winding to ground or to the secondary winding, fast-acting fuses or other overcurrent protection should be provided for safety and to prevent the MHD-EMP current from entering the facility on the ground, secondary neutral, or phase conductors. These are shown inside the transformer in Figure 5-3, but they may be either inside or outside the transformer.

For a large facility connected to a subtransmission line, delta/grounded-wye transformers are normally used in distribution substations and large industrial loads. To prevent geomagnetically induced currents on the subtransmission line, a radial or loop configuration with power supplied by one bulk power transformer at a time should be used. The subtransmission line should be configured as a ungrounded system to reduce harmonic distortion and voltage suppression at the subtransmission level. Small facilities may use single phase power. For single phase service, a delta distribution type arrangement can be employed. The two phases connected to the primary winding of the facility transformer should be balanced in a similar manner as that described for a three phase delta system. If an imbalance condition exists, some E_3 currents will flow in primary winding.

For small facilities with power requirements of 500 kVA or less, 100% power line isolation can be achieved by a rotary power conditioner consisting of a motor, flywheel, dielectric shaft, and a synchronous generator as shown in Figure 5-4. For a 500 kVA rated capacity, the installed cost is about \$130,000. This approach will provide HEMP protection and also meet TEMPEST requirements.



a. Primary distribution power line configuration



b. Isolation zone around the power line neutral ground for $\rho \geq 100 \Omega\text{-m}$ and $L \leq 30 \text{ km}$.

Figure 5-2. Modified recommendations for power system design practices.

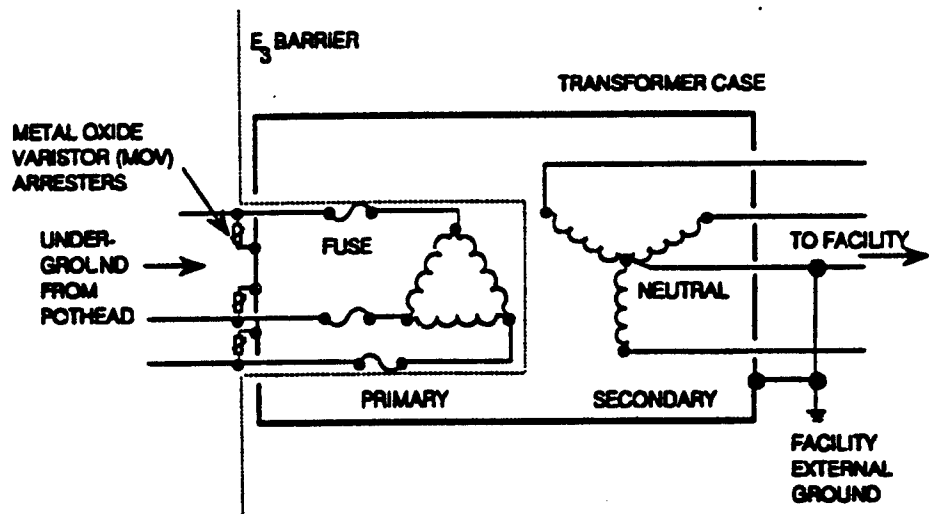


Figure 5-3. Recommended power system design practices for the facility power transformer.

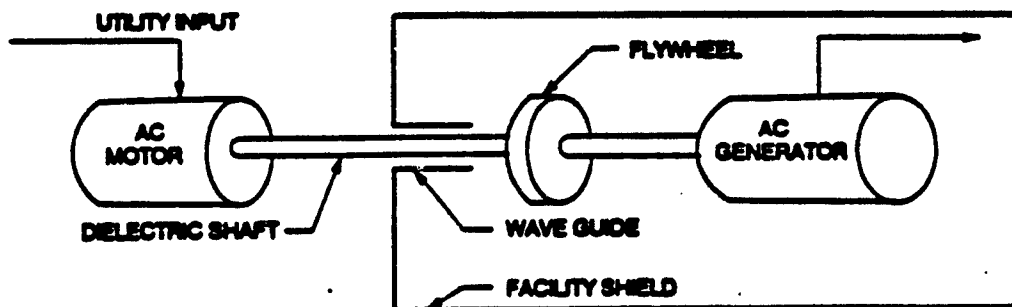


Figure 5-4. A rotary power conditioner.

5.3 OTHER CONDUCTORS.

The telephone cable, water pipes, and local power and control cables that enter the facility are potential means of transmitting MHD-EMP currents to the building. All above-ground intersite conductors should approach the facility from the same side and be electrically isolated from the facility. A portion of the telephone cable should be replaced by a fiber cable as shown in Figure 5-5. Plastic water pipes can be used in place of metal pipes and all external power should be separate from the facility. If metal pipes are used, they should be isolated from the power system ground as shown in Figure 5-2b. Fiber optic cables should be used for instrument and control functions such as the gate control, gate telephone, surveillance cameras, etc. The grounds of external equipment and metal objects should be connected to the commercial power ground and kept well separated from the facility ground. The recommended design practices for these conductors are shown in Figure 5-5. These recommendations may be relaxed after further study.

Communication cables should be also be converted to fiber optic cable to shown in Figure 5-5. If the communication cable is critical to the facility, the power supply for fiber optic converter must be protected. The converter must be provided with its own protected supply, or it must be supplied with protected power from the facility. In the latter case, precautions must be taken to prevent MHD-EMP (and other components) from entering the facility on these power leads. Small, single phase isolation transformers with protection features similar to those in Figure 5-2a may be used to supply power to the converter.

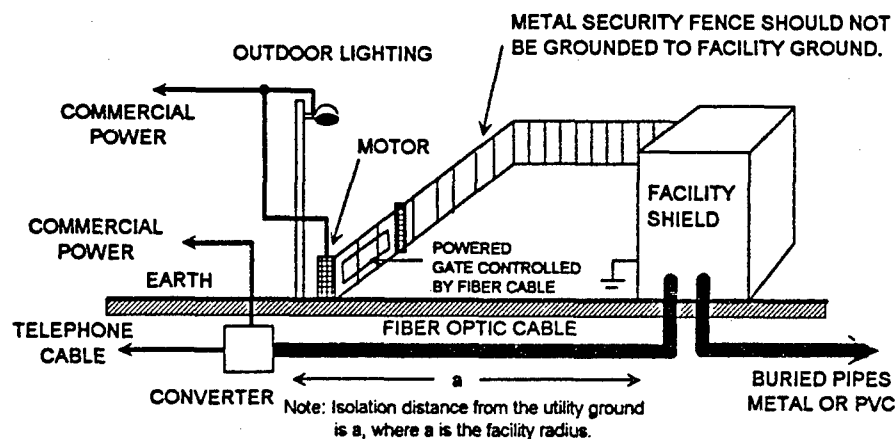


Figure 5-5. Recommended design practice for non-power line conductors.

5.4 PROTECTION AGAINST HARMONICS.

To protect facilities from the possible harmful effects of harmonic distortion on the 60 Hz power resulting from MHD-EMP or severe solar geomagnetic storms causing saturation in transformers throughout the power system, harmonic filters could be used. However, due to the large number of possible harmonics ranging from the second to the twelfth harmonic of the 60 Hz power, an effective harmonic filter would be difficult to design and relatively expensive to construct. A simpler, less costly approach is to isolate the facility from the disturbance by detecting the harmonics and activating a power transfer switch. This method of providing protection against harmonics is shown in Figure 5-6. Commercial harmonic detectors that can monitor up to the 16th harmonic of the 60 Hz fundamental frequency are available at a cost of about \$1200 [20].

Although it has been verified that saturation of power transformers can occur with dc current injection levels comparable with those predicted for MHD-EMP excitation [4], [21] the effects of such harmonics on critical loads within facilities remain largely unknown. Harmonics are known to have caused malfunctions in solid state devices, motors, disk drives, etc. [22], [23]. Consequently, harmonic effects on systems remains an open issue.

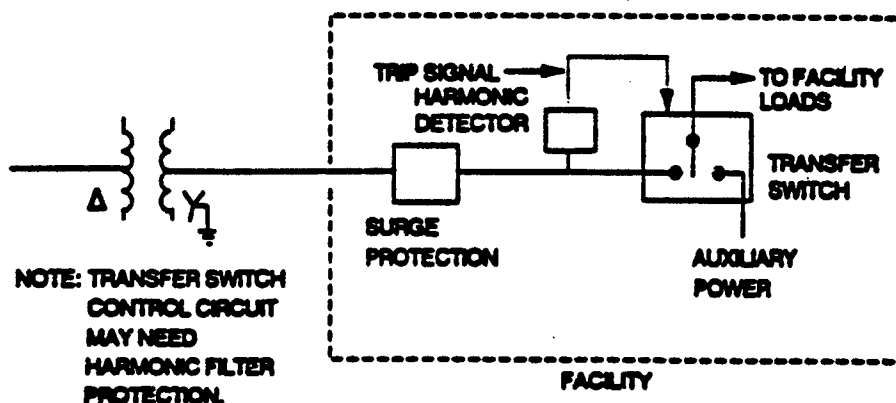


Figure 5-6. Protection against harmonics.

SECTION 6. CONCLUSIONS

6.1 SUMMARY.

MHD-EMP is a phenomena similar to that caused by solar storms, except that the geomagnetic disturbance is much more intense and occurs over a shorter period of time. In this report, the MHD-EMP environment, various coupling models and the results of several experimental simulations of this environment are summarized. More detailed information is available from the original ORNL reports. Results of these studies suggest that MHD-EMP may affect the commercial power system by causing severe harmonic distortion, voltage swings, increased reactive power demand, and ultimately, system imbalance necessitating shutdown.

The effects of harmonics and quasi-dc penetration into facilities that contain motors, computers, communication systems, and other electronic systems is presently unknown. The results of one test on a large, heavily shielded facility indicate that quasi-dc currents up to 200 A on the facility exterior appears not to be a problem. Nevertheless, the protection requirements developed early in this project assumed that this current should be reduced by a factor of 10. This may be a conservative requirement, and due to the potentially large cost implications of constructing facilities to meet this requirement, this issue deserves additional study.

This report also summarizes a number of MHD-EMP protection guidelines for ground-based facilities. Such facilities can be protected against MHD-EMP effects by isolating long conductors from the building, using the power distribution transformer as a barrier to E_3 power line currents, and addressing the harmonics generated by saturated transformers. Although many computers and electronic systems seem to be immune to harmonic distortion, harmonics can cause problems with computer disk drives, motors, viewing screens, and electronic systems with special tuning circuits. The effects of harmonic distortion of the commercial power system on critical facilities is not known. If harmonics are a problem, it appears that the most cost effective method of protecting against harmonics is to detect the presence of extreme harmonic distortion and switch the facility to auxiliary power.

6.2 RECOMMENDATIONS FOR MHD-EMP MITIGATION METHODS.

The protection recommendations in this report are based on the *assumption* that a factor of ten reduction of the MHD-EMP induced current at the facility shield is necessary. This assumption may be overly conservative. Nevertheless, for most installations where (1) the ground resistivity $\rho \geq 100 \Omega\text{-m}$, and (2) the conductor length L is restricted to be $L \leq 30 \text{ km}$, the recommended mitigation methods are within standard engineering practices. The specific mitigation recommendations are summarized as follows:

1. The facility transformer should have a three-phase delta winding on the primary (i.e., the utility) side of the transformer.
2. The power line neutral should be terminated and grounded at the last utility pole before entering the facility. This last pole should be at least a distance a from the facility power transformer, where a is one half of the longest dimension of the facility (i.e., the facility "radius"). The power line (three conductors for a three-phase system) should be connected to the facility power transformer by an underground cable in a PVC conduit. The cable terminators at the power pole should be protected by MOV surge arrestors.
3. If a grounded-wye secondary is used for the facility transformer, it should be grounded to the facility ground. The transformer case should be grounded in the same manner. The secondary main power cable should enter the facility in a metal conduit which is connected to the facility shield. The primary of the facility power should be protected against lightning and E_1 -induced transients by MOV arrestors and fuses.
4. Buried conductors such as metal pipes, lines to the security gate, etc., should be restricted from the last power pole by an isolation zone of radius a or greater.
5. Telephone and other communications lines should use a fiber optics cable without metal for a distance a or greater from the facility.
6. For cases of low earth resistance where $\rho < 100 \Omega\text{-m}$, or for very long power distribution lines where $L > 30 \text{ km}$, the more restrictive recommendations of [2] may be required. Alternatively, site-specific protection requirements can be developed using the coupling models summarized in this report.

SECTION 7

REFERENCES

1. F.M. Tesche, P.R. Barnes, and A.P. Sakis Meliopoulos, *Magnetohydrodynamic Electromagnetic Pulse (MHD-EMP) Interaction with Power Transmission and Distribution Systems*, ORNL/Sub/90-SG828/1, Martin Marietta Energy Systems, Inc., Oak Ridge Natl. Lab., Feb. 1992.
2. P.R. Barnes, F.M. Tesche, and E.F. Vance, *Mitigation of Magnetohydrodynamic Electromagnetic Pulse (MHD-EMP) Effects from Commercial Electric Power Systems*, ORNL-6709, Martin Marietta Energy Systems, Inc., Oak Ridge Natl. Lab., March 1992.
3. B.W. McConnell, et. al., *Impact of Quasi-DC Currents on Three-Phase Distribution Transformer Installations*, ORNL/Sub/89-SE912/1, Martin Marietta Energy Systems, Inc., Oak Ridge Natl. Lab., June 1992.
4. F.M. Tesche, and P.R. Barnes, *E₃ Test Observations and Lessons Learned*, Task Report Prepared for DNA Under Interagency Agreement No. 0046-C156-A1, June 19, 1992.
5. F.M. Tesche and P.R. Barnes, *Magnetohydrodynamic Electromagnetic Pulse (MHD-EMP) Interaction with Power Transmission and Distribution Systems*, paper presented at the 1992 HEART Conference, Albuquerque, NM, February 24-28, 1992, and to be published in the JRERE.
6. P.R. Barnes and E.F. Vance, *MHD-EMP Protection Guidelines*, paper presented at the 1992 HEART Conference, Albuquerque, NM, February 24-28, 1992, and to be published in the JRERE.
7. B.W. McConnell, P.R. Barnes, and F.M. Tesche, *Experimental Determination of the MHD-EMP Effects on Power Distribution Transformers*, paper presented at the 1992 HEART Conference, Albuquerque, NM, February 24-28, 1992, and to be published in the JRERE.
8. J.R. Legro, et al., *Study to Assess the Effects of Magnetohydrodynamic Electromagnetic Pulse on Electric Power Systems*, ORNL/Sub/83-43374/1/V3, Martin Marietta Energy Systems, Inc., Oak Ridge Natl. Lab., May 1985.
9. V.D. Albertson and J.A. Van Baelen, "Electric and Magnetic Fields at the Earth's Surface Due to Auroral Currents," *IEEE Trans. PAS*, Vol. PAS-89, No. 2, April 1970.
10. J.R. Legro, et al., *Study to Assess the Effects of Electromagnetic Pulse on Electric Power Systems*, ORNL/Sub/83-43374/1/V1, Martin Marietta Energy Systems, Inc., Oak Ridge Natl. Lab., Sept. 1985.

11. S. Chavin, et al., *MHD-EMP Code Simulation of Starfish*, MRC-R-516, Mission Research Corporation, Santa Barbara, CA, August, 1979.
12. Austin Research Associates, private communication with the authors, Austin, TX, March 1991.
13. J.R. Wait, *Electromagnetic Waves in Stratified Media*, Macmillan, Co. New York, 1962.
14. G. Jansen Van Beek, private communication with F.M. Tesche, Geological Survey of Canada, November 20, 1991.
15. A.W Green, private communication with F.M. Tesche, U.S. Geological Survey, November 25, 1991.
16. Reitz, J.R., and F.J. Milford, *Foundations of Electromagnetic Theory*, Addison-Wesley Co., Reading, MA, 1960.
17. Karzas, W.J., *Evaluation of Low-Frequency Current Flow as a Function of Grounding Distance*, Technical Memorandum, Metatech Corp. Santa Monica, CA, September 16, 1990.
18. T.J. Zwolinski, *General Test Plan for the FEMA Facility at Olney, MD*, MRC/COS-R-1286, Mission Research Corp., April 8, 1992.
19. High-Altitude Electromagnetic Pulse (HEMP) Protection for Ground-Based C⁴I Facilities Performing Critical, Time-Urgent Missions, MIL-STD-188-125, U.S. Department of Defense, June 26, 1990.
20. Data sheet for HD-510 Harmonic Trigger, Rochester Instrument Systems, Rochester N.Y.
21. J.G. Kappenman, *Transformer DC Excitation Field Test and Results*, Special Panel Session Report 90TH0291-PWR, IEEE PES Summer Meeting, July, 12, 1989.
22. J.S. Subjak, Jr. and J.S. McQuilkin, "Harmonics - Causes, Effects, Measurements, and Analysis: an Update", *IEEE Trans. Ind. Aps.*, Vol. 26, No.6, Nov./Dec. 1990.
23. B. Brotschi and A.C. Tucker, "Nonlinear Loading of an AC Mains Network Investigated", *EMC 91- Direct to Compliance*, Conference Volume, 13-14 Feb, 1991, London, UK.

Note: The ORNL reports referenced in this document are available to the public from the National Technical Information Service, U.S. Department of Commerce, 5285 Port Royal Rd., Springfield, VA 22161.

APPENDIX

LIST OF ACRONYMS, ABBREVIATIONS AND SYMBOLS

A	amperes
ac	alternating current
dc	direct current
DNA	Defense Nuclear Agency
DoD	U.S. Department of Defense
DOE	Department of Energy
E ₁	the early-time HEMP environment
E ₂	the intermediate-time HEMP environment
E ₃	the MHD-EMP late-time HEMP
EMP	electromagnetic pulse
ESA	electric surge arrestor
FEMA	Federal Emergency Management Agency
GMD	geomagnetic disturbance
H	Henry
HEMP	high-altitude electromagnetic pulse
Hz	hertz
I	current
kV	kilovolts
kVA	kilovolts times amperes
m	meter
MHD-EMP	magnetohydrodynamic electromagnetic pulse
MOV	metal oxide varistor
MRC	Mission Research Corp.
ORNL	Oak Ridge National Laboratory
POE	points of entry
PVC	polyvinyl chloride
S	siemens (Mhos)
UPS	uninterruptable power supply
V	volts
VAR	volts × amperes reactive (reactive power)
Ω	ohms

DISTRIBUTION LIST

DNA-TR-82-101

DEPARTMENT OF DEFENSE

ARMED FORCES RADIOBIOLOGY RSCH INST
ATTN: DR M R LANDAUER BHS

ASSISTANT TO THE SECRETARY OF DEFENSE
ATTN: EXECUTIVE ASSISTANT
ATTN: E CHASE

DEFENSE INFORMATION SYSTEMS AGENCY
ATTN: COMMANDER

DEFENSE INTELLIGENCE AGENCY
ATTN: J REMPEL
ATTN: DW-4
ATTN: DT-SA R BURGER
ATTN: VP-TPO

DEFENSE NUCLEAR AGENCY
ATTN: OPNA
ATTN: RAAE K SCHWARTZ
5 CY ATTN: RAE LTC R J LAUNSTEIN
2 CY ATTN: TTTL

DEFENSE TECHNICAL INFORMATION CENTER
2 CY ATTN: DTIC/OC

FIELD COMMAND DEFENSE NUCLEAR AGENCY
2 CY ATTN: FCTT W SHoup
2 CY ATTN: NMOP LT COL R GWYN
ATTN: TTTT LTCOL GIFFORD

NATIONAL DEFENSE UNIVERSITY
ATTN: NWC0

NET ASSESSMENT
ATTN: DOCUMENT CONTROL

USSTRATCOM/J531T
ATTN: JPEN MAJ J ROBBINS

DEPARTMENT OF THE ARMY

ARMY RESEARCH LABORATORIES
ATTN: TECH LIB
ATTN: M SMITH
ATTN: SLCHD-NW
ATTN: SLCHD-NW
ATTN: SLCHD-NW-CS LOU JASPER JR
ATTN: SLCHD-NW-E E L PATRICK
2 CY ATTN: SLCHD-NW-E R L ATKINSON
ATTN: SLCHD-NW-EP
ATTN: SLCHD-NW-RP
ATTN: SLCHD-NW-TN
ATTN: SLCHD-NW-TN G MERKEL
ATTN: W PATTERSON

DEP CH OF STAFF FOR OPS & PLANS
ATTN: DAMO-ODW

NUCLEAR EFFECTS DIVISION
ATTN: STEWS-NE J MEASON

PEO COMMUNICATION
ATTN: J BOWDEN
ATTN: V PHILLIPUK

U S ARMY ATMOSPHERIC SCIENCES LAB
ATTN: SLCAS-AS

U S ARMY BALLISTIC RESEARCH LAB
ATTN: SLCBR-SS-T
ATTN: SLCBR-TB-B G BULMASH
ATTN: SLCBR-VL

U S ARMY BELVOIR RD&E CTR
ATTN: STRBE-H WEN H CHEN

U S ARMY ENGINEER DIV HUNTSVILLE
ATTN: CEHND-SY J LOYD
ATTN: HNDED-SY

U S ARMY NUCLEAR & CHEMICAL AGENCY
ATTN: MONA-NU A RENNER
ATTN: MONA-NU DR D BASH

U S ARMY SPACE & STRATEGIC DEFENSE CMD
ATTN: CSSD-SL

U S ARMY STRATEGIC SPACE & DEFENSE CMD
ATTN: CSSD-SA-E

U S ARMY TEST & EVALUATION COMMAND
ATTN: TECHNICAL LIBRARY SIF

U S ARMY WAR COLLEGE
ATTN: LIBRARY

US ARMY MATERIEL SYS ANALYSIS ACTVY
ATTN: AMXSY-CR

DEPARTMENT OF THE NAVY

NAVAL AIR SYSTEMS COMMAND
ATTN: AIR 5181

NAVAL AIR TEST CENTER
ATTN: SY84

NAVAL CIVIL ENGINEERING LABORATORY
ATTN: L72 JAMES BROOKS

NAVAL ELECTRONIC ENGINEERING ACTIVITIES PACIFIC
ATTN: S KUBA

NAVAL OCEAN SYSTEMS CENTER
ATTN: CODE 824 W KORDELA

NAVAL POSTGRADUATE SCHOOL
ATTN: CODE 1424 LIBRARY
ATTN: X MARYAMA
ATTN: PROF DONALD L WALTERS

NAVAL RESEARCH LABORATORY
ATTN: CODE 5227 RESEARCH REPORT

NAVAL SEA SYSTEMS COMMAND

ATTN: J GANN
ATTN: NAVSEA-05R24

NAVAL SURFACE WARFARE CENTER

ATTN: CODE H23 J PARTAK
ATTN: CODE H25 G BRACKETT
ATTN: CODE R41
ATTN: CODE 425
ATTN: WO/H25 N STETSON

NAVAL SURFACE WARFARE CENTER

ATTN: CODE H-21

NAVAL UNDERWATER SYSTEMS CENTER

ATTN: CODE 3431 DAVID S DIXON

OFFICE OF CHIEF OF NAVAL OPERATIONS

ATTN: NOP 098
ATTN: NOP 551
ATTN: NOP 941F
ATTN: NUC AFFAIRS & INTL NEGOT BR
ATTN: N88OE

DEPARTMENT OF THE AIR FORCE

AIR FORCE CTR FOR STUDIES & ANALYSIS

ATTN: AFSAA/SAI

AIR FORCE SPACE COMMAND

ATTN: DEES/D C DE MIO

AIR FORCE SPACE COMMAND

ATTN: 4 SCS/DW

AIR UNIVERSITY LIBRARY

ATTN: AUL-LSE

BOLLING AFB

ATTN: LEEU R FERNANDEZ

OKLAHOMA CITY AIR LOGISTICS CTR/TIES

ATTN: TIESW 1LT A POPOVICH

SPACE DIVISION/IN

ATTN: IND

DEPARTMENT OF ENERGY

LAWRENCE LIVERMORE NATIONAL LAB

ATTN: J SEFCIK
ATTN: S YOUNGER

LOS ALAMOS NATIONAL LABORATORY

ATTN: REPORT LIBRARY

OAK RIDGE NATIONAL LABORATORY

2 CY ATTN: B MCCONNELL
2 CY ATTN: E VANCE
2 CY ATTN: F TESCHE
2 CY ATTN: R BARNES

SANDIA NATIONAL LABORATORIES

ATTN: TECH LIB 3141

U S DEPT OF ENERGY IE-24

ATTN: J BUSSE

OTHER GOVERNMENT

FEDERAL EMERGENCY MANAGEMENT AGENCY

ATTN: R GATES

DEPARTMENT OF DEFENSE CONTRACTORS

ALLIED-SIGNAL, INC

ATTN: DOCUMENT CONTROL

BDM FEDERAL INC

ATTN: ADV SYSTEM TECH DIV
ATTN: E DORCHAK

BDM FEDERAL INC

ATTN: B TORRES
ATTN: L O HOEFT
ATTN: LIBRARY
ATTN: R HUTCHINS
ATTN: B PLUMMER

BELL HELICOPTER TEXTRON, INC

ATTN: HEINZ FABER

BOEING CO

ATTN: D GERMAN
ATTN: D EGELKROUT
ATTN: D CHAPMAN
ATTN: F LENNING

BOEING TECHNICAL & MANAGEMENT SVCS, INC

ATTN: ARNOLD D BAKER

BOOZ ALLEN & HAMILTON INC

ATTN: D VINCENT
ATTN: T J ZWOLINSKI

BOOZ-ALLEN & HAMILTON, INC

ATTN: TECHNICAL LIBRARY

COMPUTER SCIENCES CORP

ATTN: A SCHIFF

E-SYSTEMS, INC

ATTN: TECH INFO CTR
ATTN: W GETSON

EG&G SPECIAL PROJECTS INC

ATTN: J GILES

EG&G WASH ANALYTICAL SVCS CTR, INC

ATTN: D HIGHTOWER

EG&G WASH ANALYTICAL SVCS CTR, INC

ATTN: R BRENT JACOBS

ELECTRO-MAGNETIC APPLICATIONS, INC

ATTN: TECH LIBRARY

FAIRCHILD SPACE COMPANY

ATTN: R CARPENTER

FALCON ASSOCIATES, LTD

ATTN: T NEIGHBORS

GENERAL ELECTRIC COMPANY

ATTN: D TASCA
ATTN: J KLISCH

GENERAL RESEARCH CORP
ATTN: W NAUMANN

HONEYWELL SYSTEMS & RESEARCH CENTER
ATTN: T CLARKIN

INT RESEARCH INSTITUTE
ATTN: J STANGEL

INSTITUTE FOR DEFENSE ANALYSES
ATTN: CLASSIFIED LIBRARY
ATTN: TECH INFO SERVICES

JAYCOR
ATTN: CYRUS P KNOWLES
ATTN: E WEMAAS
ATTN: M SCHULTZ JR

JAYCOR
ATTN: E PETERSON

KAMAN SCIENCES CORP
ATTN: C EKLUND

KAMAN SCIENCES CORP
ATTN: DASAC
ATTN: E CONRAD

KAMAN SCIENCES CORPORATION
ATTN: D MCLEMORE

KAMAN SCIENCES CORPORATION
ATTN: DASAC
ATTN: R RUTHERFORD

KEARFOTT GUIDANCE AND NAVIGATION CORP
ATTN: J D BRINKMAN

LITTON SYSTEMS, INC
ATTN: J SKAGGS

LOCKHEED MISSILES & SPACE CO, INC
ATTN: G LUM
ATTN: TECH INFO

LOCKHEED SANDERS, INC
ATTN: BRIAN G CARRIGG

LOGICON R & D ASSOCIATES
ATTN: DOCUMENT CONTROL
ATTN: G K SCHLEGEL

LOGICON R & D ASSOCIATES
ATTN: E QUINN

LOGICON R & D ASSOCIATES
ATTN: J P CASTILLO
ATTN: W S KEHRER

LTV AEROSPACE & DEFENSE COMPANY
2 CY ATTN: LIBRARY EM-08

MCDONNELL DOUGLAS CORP
ATTN: J W MCCORMACK

METATECH CORP
ATTN: C JONES

MISSION RESEARCH CORP
ATTN: EMP GROUP
ATTN: J GILBERT
ATTN: N CARRON
ATTN: N CARRON
ATTN: TECH INFO CENTER

MISSION RESEARCH CORP
ATTN: A CHODOROW

MISSION RESEARCH CORP
ATTN: J L BELL
ATTN: J G CURRY

MITRE CORPORATION
ATTN: M FITZGERALD

MITRE CORPORATION
ATTN: DIRECTOR

PACIFIC-SIERRA RESEARCH CORP
ATTN: H BRODE

PHOTOMETRICS, INC
ATTN: I L KOPSKY

PHYSICS INTERNATIONAL CO
ATTN: C GILMAN
ATTN: C STALLINGS
ATTN: J NAFF

PHYSITRON INC
ATTN: J HARPER

PHYSITRON INC
ATTN: MARION ROSE

RAND CORP
ATTN: ENGR & APPLIED SCIENCES DEPT
ATTN: TECH LIBRARY

RESEARCH TRIANGLE INSTITUTE
ATTN: M SIMONS

ROCKWELL INTERNATIONAL CORP
ATTN: J C ERB
ATTN: P BELL

ROCKWELL INTERNATIONAL CORP
ATTN: P BELL

S-CUBED
ATTN: J KNIGHTEN
ATTN: LLOYD DUNCAN
ATTN: R W STEWART

SCIENCE & ENGRG ASSOCIATES, INC
ATTN: R M SMITH

SCIENCE APPLICATIONS INTL CORP
ATTN: J RETZLER

SCIENCE APPLICATIONS INTL CORP
ATTN: J ERLER
ATTN: W ADAMS
ATTN: W CHADSEY
ATTN: W LAYSON

DNA-TR-92-101 (DL CONTINUED)

SCIENCE APPLICATIONS INTL CORP
ATTN: T NEIGHBORS

SOL TELECOMMUNICATIONS SERVICES
ATTN: S CLARK

SRI INTERNATIONAL
ATTN: E VANCE
ATTN: W GRAF

TELEDYNE BROWN ENGINEERING
ATTN: LEWIS T SMITH
ATTN: RONALD E LEWIS

TRW
ATTN: M J TAYLOR

TRW INC
ATTN: LIBRARIAN

UNISYS CORPORATION-DEFENSE SYSTEMS
ATTN: TECHNICAL LIBRARY

UNITED TECHNOLOGIES CORP
ATTN: R D TOTTON

WESTINGHOUSE ELECTRIC CORP
ATTN: D CARRERA
ATTN: S LAKHAVANI

FOREIGN

DEFENCE RESEARCH ESTABLISHMENT OTTAWA
ATTN: S KASHYAP